PL-TR-92-2125

ANALYSIS AND TESTING OF HIGH-FREQUENCY REGIONAL SEISMIC DISCRIMINANTS

Jay J. Pulli
Paul S. Dysart

Radix Systems Inc
6 Taft Court
Rockville, MD 20850-1307

30 September 1992

Final Report
27 August 1991-31 July 1992

APPROVED FOR PUBLIC RELEASE; DISTRIBUTION UNLIMITED

PHILLIPS LABORATORY
Directorate of Geophysics
AIR FORCE MATERIEL COMMAND
HANSCOM AIR FORCE BASE, MA 01731-5000

SPONSORED BY
Defense Advanced Research Projects Agency
Nuclear Monitoring Research Office
ARPA ORDER NO. 5307

MONITORED BY
Phillips Laboratory
Contract No. F19628-91-C-0111

The views and conclusions contained in this document are those of the authors and should not be interpreted as representing the official policies, either expressed or implied, of the Defense Advanced Research Projects Agency or the U.S. Government.

This technical report has been reviewed and is approved for publication.

JAMES F. LEWKOWICZ
Contract Manager
Solid Earth Geophysics Branch
Earth Sciences Division

JAMES F. LEWKOWICZ
Branch Chief
Solid Earth Geophysics Branch
Earth Sciences Division

DONALD H. ECKHARDT, Director
Earth Sciences Division

This report has been reviewed by the ESD Public Affairs Office (PA) and is releasable to the National Technical Information Service (NTIS).

Qualified requestors may obtain additional copies from the Defense Technical Information Center. All others should apply to the National Technical Information Service.

If your address has changed, or if you wish to be removed from the mailing list, or if the addressee is no longer employed by your organization, please notify PL/IMA, Hanscom AFB, MA 01731-5000. This will assist us in maintaining a current mailing list.

Do not return copies of this report unless contractual obligations or notices on a specific document requires that it be returned.

REPORT DOCUMENTATION PAGE

Form Approved
OMB No. 0704-0188

1. AGENCY USE ONLY (Leave blank)	2. REPORT DATE	3. REPORT TYPE AND DATES COVERED
	30 September 1992	Final (27 August 1991-31 July 1992)

4. TITLE AND SUBTITLE
Analysis and Testing of High-Frequency Regional Seismic Discriminants

5. FUNDING NUMBERS
PE 62714E
PR 0A10 TA DA WU AG

Contract F19628-91-C-0111

6. AUTHOR(S)
Jay J. Pulli
Paul S. Dysart

7. PERFORMING ORGANIZATION NAME(S) AND ADDRESS(ES)
Radix Systems, Inc
6 Taft Court
Rockville, MD 20850-1307

8. PERFORMING ORGANIZATION REPORT NUMBER

9. SPONSORING/MONITORING AGENCY NAME(S) AND ADDRESS(ES)
Phillips Laboratory
Hanscom AFB, MA 01731-5000

Contract Manager: James Lewkowicz/GPEH

10. SPONSORING/MONITORING AGENCY REPORT NUMBER
PL-TR-92-2125

11. SUPPLEMENTARY NOTES

12a. DISTRIBUTION/AVAILABILITY STATEMENT
Approved for public release; distribution unlimited

12b. DISTRIBUTION CODE

13. ABSTRACT (Maximum 200 words)
The objective of this research was to test the applicability of artificial neural networks (ANN's) for seismic event identification. Research has focused on 101 small events within regional distances of the NORESS array for which independent source identifications are available. 12 signal parameters were extracted from the *P*-, *S*-, and *Lg*-waves of each event. A number of descriptive statistics were calculated for the purpose of understanding the parameter dataspace. These included means, variances, tests for normality, and cross-correlations between signal parameters. A Stepwise Discriminant Analysis was performed to eliminate parameters which do not contribute to the identification. The 6 most important parameters were the *Pn/Lg* spectral ratio from 5-10 Hz, the mean cepstral variance, the *Pn/Sn* wideband spectral ratio, the *Pn/Lg* spectral ratio from 2-5 Hz, the *Pn/Sn* spectral ratio from 2-5 Hz, and the *Pn/Lg* spectral ratio from 10-20 Hz. Principal Components Analysis was applied to the reduced parameter dataset to aid in the design of the ANN. Three principal components account for more than 85% of the data variance, providing a useful guide to the appropriate hidden layer dimensionality. The final ANN design consisted of an input layer with 12 units, a single hidden layer with 3 units, and an output layer of 1 unit. The ANN was trained using the backpropagation learning algorithm. The ANN correctly identified all but 2 of the 101 events; 2 explosions were misclassified as earthquakes. Experiments were also conducted using inputs from 1, 5, 10, 15, 20, and 25 NORESS elements as a means of testing the ANN sensitivity to SNR. Identification performance increased from 77% for 1 element to 98% for 25 elements.

14. SUBJECT TERMS
Regional seismic discriminants
Artificial neural networks
Principal components analysis
Back propagation

15. NUMBER OF PAGES
72

16. PRICE CODE

17. SECURITY CLASSIFICATION OF REPORT	18. SECURITY CLASSIFICATION OF THIS PAGE	19. SECURITY CLASSIFICATION OF ABSTRACT	20. LIMITATION OF ABSTRACT
Unclassified	Unclassified	Unclassified	SAR

Table of Contents

List of Figures

List of Tables

1. Introduction

1.1 Overview of the Seismic Identification Problem

A consequence of the breakup of the former Soviet Union is the change in priority of seismic monitoring efforts for the detection of underground nuclear tests. The detection target has shifted from large explosions at known test sites to small explosions worldwide. Specifically, DARPA is focusing its efforts on monitoring countries identified as potential proliferators at the 1 kiloton (kt) level (m_b approximately 2.5), as well as worldwide explosions at the 10-kt level (m_b approximately 3.0 - 3.5). These goals were recently outlined at the DARPA Seismic Identification Workshop, held on May 18-19, 1992 (Blandford et al., 1992)

Seismic monitoring at these low levels implies a multi-fold increase in the volume of data which must be analyzed. Not only does the number of natural seismic events increase exponentially with decreasing magnitude (the familiar $Log(N) = A - BM$ relation), but the monitoring threshold also includes the majority of worldwide mining explosions. This data handling problem has led to the development of systems such as the Intelligent Monitoring System (IMS) (Bache et al., 1990; Bratt et al., 1990) which automatically detects and locates regional seismic events from a network of seismic arrays and three-component stations. The IMS is an *expert system* based processor, which uses decision rules based on the experience of trained seismic analysts.

The event identification problem, which is generally undertaken after the event has been detected and located, is usually accomplished manually by a trained seismic analyst. The analyst may accomplish this task by visual pattern recognition of the waveforms or by a number of signal processing techniques. This identification problem can be defined in a number of ways: earthquake vs. explosion; earthquake vs. chemical explosion vs. nuclear explosion; earthquake vs. specific mine vs. specific test site. No matter which definition is used, it is clear that the next development in automated seismic processing must be event identification. However, unlike the detection and location problems which are well understood, the identification problem has been an elusive target, especially at regional distances. Proposed seismic discriminants may work in one geographic or tectonic area but not another. Consequently, the automation of seismic identification has been an extremely difficult problem, because the formal methodology for even manual identification has yet to be developed.

A possible solution to the identification problem may lie in modern machine learning techniques. These techniques use examples of identified events for self-training, as opposed to expert systems which must be programmed with known rules. One example of a machine learning technique which is gaining wide acceptance is the artificial neural network (ANN) (c.f. Lippman, 1987). ANN's have recently been applied to a number of pattern recognition and classification

problems, such as sonar signal classification, voice recognition, image recognition, and time series prediction.

1.2 Project Objectives

The objective of this research project is to test the applicability of machine learning techniques to the problem of regional seismic event identification. The testbed for this effort will be waveforms for seismic events recorded by the NORESS array in southern Norway. The NORESS array was selected because it is a source of high-quality digital data in an area which includes both natural earthquakes and many mines. Independent events identifications are also available from local sources such as the Bergen Seismological Observatory and the University of Helsinki Institute of Seismology.

The specific tasks involved in this research effort are as follows:

- Select a database of previously identified small seismic events which includes both earthquakes and explosions.
- Dearchive the waveform data for these events from the databases at DARPA's Center for Seismic Studies (CSS).
- Select a set of signal parameters and discriminants to be extracted from the seismic waveforms.
- Graphically review the waveform data for such problems as spikes, data dropouts, and noise.
- Graphically select the time windows of the P_n, S_n, and L_g waves for each event, and compute the selected signal parameters for each time window.
- Statistically examine the signal parameters as a guide to the design of the backpropagation ANN.
- Train and test the ANN and assess the network's performance.

Section 2 of this report discusses the event database used for training the backpropagation ANN's. Section 3 includes the description of the selected signal parameters, the data processing to extract the parameters, and the analysis of the signal parameters. Section 4 discusses the design, training, and testing of the ANN's. Section 5 summarizes the results of this research project.

2. The Event Database

2.1 Database Requirements

The compilation of the event database (often called the *training set* or *ground truth* in the language of neural networks) is generally the most difficult and time consuming step in any machine learning problem. The primary constraint of this step is that the training set be accurate, that is, that the earthquakes and explosions be accurately and positively identified. There are certainly many levels of identification truth which can be stated. The top level of certainty in the case of an explosion would be for a representative to be present at the site of detonation. Somewhat below this level would be a report from the mine which correlated with the seismic observation. Below this would be an independent identification published in a seismic bulletin from the source area.

Beyond the ground truth problem, a good training set should include data which spans the entire domain. In terms of our seismic identification application, this mean having a dataset of explosions and earthquakes which cover the magnitude range of interest as well as all distances and azimuths. The later means that all cases of propagation effects would be spanned by the data. Clearly in *passive* experiments such as seismic monitoring, one must accept the distribution of natural seismicity and man-made mining sites present in the area of study. In the case of the area surrounding the NORESS array, this means that most mining explosions are either to the east, south, or west of the array. Most earthquakes are either to the northwest, west or south of the array.

2.2 Strategy for Event Selection

Our strategy in the selection of the training database was to examine the local seismic bulletins from the Bergen Seismological Observatory, the University of Helsinki Institute of Seismology, and the U.S. Geological Survey's Monthly Preliminary Determination of Epicenters (PDE) list. The PDE was especially useful for selecting earthquakes in the Norwegian and Greenland Seas. Over 500 *origins* were selected for examination, but that number shrank to 101 useful events by the time the data were dearchived (if the waveforms were available) and quality control checked (see Section 3.2).

Figure 1 shows a map of the study area with the location of the NORESS array and the locations of the training events. Origin information for all of these events is given in *Table 1*. The magnitude distribution of these events is shown in *Figure 2*. Half of the events have no associated magnitude calculation, hence the peak near magnitude zero. For the events with an associated magnitude, the mean of the distribution is 2.5 . The distance distribution, shown in *Figure 3*, shows peaks at 400

km and 900 km, with a few events at a distance of about 2500 km. The azimuth distribution, seen in *Figure 4*, shows peaks to the west and east of the array. Events to the west include both earthquakes and mining explosions along coastal Norway, whereas the events to the east are primarily mining explosions in Estonia.

Since this research effort began, at least two independent investigators have worked to establish a database of training events for neural network development and testing. Sereno and Patnaik (1991) compiled a database of origins and associated waveforms for nearly 300 events recorded by the NORESS and ARCESS arrays. This database has been used as the basis for neural network studies conducted by Lacoss et al (1992). Lately, Grant and Coyne (1992) have undertaken an effort to compile a database of ground truth for seismic identification research which includes relational information that is much more specific than "explosion" or "earthquake". Their database includes tracing information such as the original source of the identification and whether or not the explosion was confirmed by quarrying operation records. The availability of these databases means that future studies in seismic identification can proceed much more rapidly now that the tedious job of database compilation has been assumed by full time, independent efforts.

Table 1. Training Database of Origins

Lat.	Lon.	Depth	Mag.†	Jdate	Date	O.T.	Class
61.301	7.840	10.000	-1.00	1991006	1/06/1991	6:29:18.80	Earthquake
65.370	6.219	10.000	-1.00	1991013	1/13/1991	2:22:09.30	Earthquake
61.896	3.995	10.000	-1.00	1991023	1/23/1991	15:45:36.40	Earthquake
62.427	5.370	10.000	-1.00	1991033	2/02/1991	18:40:57.30	Earthquake
59.894	8.928	0.000	-1.00	1991066	3/07/1991	14:40:13.40	Explosion
57.329	9.512	10.000	-1.00	1991070	3/11/1991	21:09:04.50	Earthquake
58.016	7.331	10.000	-1.00	1991076	3/17/1991	2:59:58.30	Earthquake
61.641	4.386	10.000	-1.00	1991086	3/27/1991	2:24:32.10	Earthquake
70.990	-5.971	10.000	-1.00	1991089	3/30/1991	0:44:14.70	Earthquake
62.032	2.800	10.000	-1.00	1991104	4/14/1991	15:28:40.60	Explosion
60.316	1.573	18.000	-1.00	1991115	4/25/1991	16:27:44.90	Earthquake
61.410	3.814	10.000	-1.00	1991144	5/24/1991	15:19:39.70	Earthquake
59.814	6.064	10.000	-1.00	1991146	5/26/1991	9:00:16.20	Earthquake
72.961	12.309	10.000	5.40	1991183	7/02/1991	21:24:03.80	Earthquake
39.790	20.560	10.000	-1.00	1985106	4/16/1985	12:46:45.10	Earthquake
59.300	28.100	0.000	2.30	1985298	10/25/1985	12:03:47.00	Explosion
61.100	4.920	0.000	-1.00	1985300	10/27/1985	4:36:43.00	Earthquake
58.340	6.430	0.000	1.90	1985312	11/08/1985	14:18:52.40	Explosion
57.800	7.200	0.000	2.10	1985313	11/09/1985	14:42:45.40	Explosion
62.000	7.700	0.000	2.00	1985313	11/09/1985	18:20:48.00	Explosion
58.340	6.430	0.000	1.80	1985317	11/13/1985	14:11:05.80	Explosion
59.300	28.100	0.000	2.30	1985317	11/13/1985	12:07:48.00	Explosion
57.800	6.700	0.000	2.10	1985324	11/20/1985	22:10:43.80	Explosion
58.530	6.040	0.000	2.10	1985324	11/20/1985	22:24:52.40	Explosion

58.500	4.900	0.000	2.10	1985324	11/20/1985	22:57:08.20	Explosion
58.800	4.700	0.000	2.10	1985324	11/20/1985	23:10:45.90	Explosion
57.500	7.000	0.000	2.10	1985324	11/20/1985	23:17:26.70	Explosion
57.500	6.900	0.000	2.10	1985324	11/20/1985	23:23:08.00	Explosion
57.700	5.030	0.000	1.40	1985325	11/21/1985	14:18:13.00	Explosion
54.800	6.500	0.000	2.80	1985325	11/21/1985	14:48:07.10	Explosion
58.370	12.360	0.000	-1.00	1985325	11/21/1985	9:16:30.00	Explosion
59.400	25.100	0.000	2.10	1985327	11/23/1985	13:06:15.00	Explosion
59.730	5.710	15.000	-1.00	1985331	11/27/1985	4:53:32.80	Earthquake
59.400	28.500	0.000	3.00	1985344	12/10/1985	12:05:46.00	Explosion
60.380	1.900	15.000	-1.00	1985357	12/23/1985	2:35:08.30	Earthquake
58.700	26.000	0.000	2.60	1985359	12/25/1985	13:19:01.00	Explosion
59.400	28.500	0.000	4.18	1985361	12/27/1985	12:16:06.20	Explosion
68.400	11.600	0.000	3.10	1985365	12/31/1985	6:58:24.00	Earthquake
58.340	6.430	0.000	2.30	1986017	1/17/1986	14:10:58.00	Explosion
59.300	24.400	0.000	-1.00	1986035	2/04/1986	14:22:57.00	Explosion
62.800	4.860	0.000	4.70	1986036	2/05/1986	17:53:16.00	Earthquake
67.100	20.600	0.000	2.70	1986037	2/06/1986	16:29:55.00	Explosion
59.300	28.100	0.000	-1.00	1986037	2/06/1986	12:22:04.00	Explosion
63.900	28.300	0.000	1.60	1986038	2/07/1986	14:06:11.00	Explosion
64.700	30.700	0.000	-1.00	1986038	2/07/1986	11:00:01.00	Explosion
59.400	28.500	0.000	-1.00	1986041	2/10/1986	12:41:46.00	Explosion
59.400	28.500	0.000	-1.00	1986045	2/14/1986	12:10:21.00	Explosion
67.100	20.600	0.000	-1.00	1986045	2/14/1986	16:44:08.00	Explosion
59.300	27.200	0.000	-1.00	1986049	2/18/1986	10:46:16.00	Explosion
64.700	30.700	0.000	-1.00	1986049	2/18/1986	12:45:50.00	Explosion
62.760	5.290	15.000	-1.00	1986057	2/26/1986	2:11:44.60	Earthquake
59.500	26.500	0.000	-1.00	1986064	3/05/1986	12:13:19.00	Explosion
60.630	2.580	15.000	-1.00	1986064	3/05/1986	13:02:05.00	Earthquake
61.670	2.580	15.000	-1.00	1986067	3/08/1986	16:21:17.00	Earthquake
59.300	28.100	0.000	-1.00	1986069	3/10/1986	12:02:09.00	Explosion
62.810	4.910	15.000	-1.00	1986069	3/10/1986	4:20:04.00	Earthquake
59.300	28.100	0.000	-1.00	1986070	3/11/1986	12:02:28.00	Explosion
59.500	26.500	0.000	-1.00	1986071	3/12/1986	11:07:21.00	Explosion
59.400	28.500	0.000	-1.00	1986071	3/12/1986	12:01:38.00	Explosion
59.400	28.500	0.000	-1.00	1986078	3/19/1986	12:06:40.00	Explosion
61.660	4.530	15.000	-1.00	1986089	3/30/1986	3:22:37.70	Earthquake
56.460	11.970	0.000	3.70	1986091	4/01/1986	9:56:47.00	Earthquake
68.300	11.600	0.000	-1.00	1986094	4/04/1986	22:43:06.00	Earthquake
61.840	4.880	15.000	-1.00	1986097	4/07/1986	0:34:37.00	Earthquake
59.220	1.420	15.000	-1.00	1986108	4/18/1986	0:44:13.70	Earthquake
54.700	33.800	0.000	4.50	1986133	5/13/1986	9:23:44.00	Earthquake
61.460	4.080	15.000	-1.00	1986154	6/03/1986	14:30:04.50	Earthquake
60.200	29.900	0.000	3.30	1986163	6/12/1986	9:30:55.10	Explosion
61.670	3.850	15.000	-1.00	1986166	6/15/1986	15:01:07.20	Earthquake
59.400	28.500	0.000	-1.00	1986168	6/17/1986	12:12:07.00	Explosion
59.400	28.500	0.000	-1.00	1986169	6/18/1986	11:05:08.00	Explosion
59.310	6.540	0.000	-1.00	1986170	6/19/1986	3:55:08.70	Explosion
61.470	3.920	15.000	-1.00	1986171	6/20/1986	22:07:53.50	Explosion
61.880	5.100	15.000	-1.00	1986177	6/26/1986	4:06:21.30	Earthquake
59.280	6.760	15.000	-1.00	1986178	6/27/1986	3:49:46.20	Earthquake
59.300	28.100	0.000	-1.00	1986185	7/04/1986	11:13:27.00	Explosion
37.800	20.870	10.000	-1.00	1986189	7/08/1986	16:15:03.70	Earthquake
58.400	14.200	0.000	4.30	1986195	7/14/1986	13:50:32.00	Earthquake
61.100	29.900	0.000	-1.00	1986195	7/14/1986	14:30:27.00	Explosion

59.990	5.340	15.000	-1.00	1986222	8/10/1986	5:01:03.90	Earthquake
62.820	4.980	15.000	-1.00	1986228	8/16/1986	4:24:36.00	Earthquake
60.820	2.930	15.000	-1.00	1986244	9/01/1986	22:11:25.60	Earthquake
60.790	4.230	15.000	-1.00	1986273	9/30/1986	20:02:46.80	Earthquake
61.970	2.330	15.000	-1.00	1986283	10/10/1986	19:56:30.80	Earthquake
61.460	3.290	15.000	-1.00	1986299	10/26/1986	11:45:06.20	Earthquake
61.720	3.270	15.000	-1.00	1986299	10/26/1986	11:57:03.50	Earthquake
60.810	3.040	15.000	-1.00	1986302	10/29/1986	21:05:00.70	Earthquake
73.736	9.080	10.000	4.70	1986327	11/23/1986	3:30:40.00	Earthquake
43.290	25.990	0.000	-1.00	1986342	12/08/1986	14:44:27.20	Earthquake
72.960	4.800	10.000	4.70	1986346	12/12/1986	16:33:36.00	Earthquake
39.810	19.720	0.000	-1.00	1986351	12/17/1986	21:18:31.50	Earthquake
43.280	26.010	0.000	-1.00	1986352	12/18/1986	17:16:15.80	Earthquake
39.480	20.520	0.000	-1.00	1987067	3/08/1987	17:42:20.70	Earthquake
58.000	56.000	0.000	-1.00	1987109	4/19/1987	4:00:07.00	Earthquake

† Magnitude values of -1.00 indicate no magnitude available.

Locations of Training Events

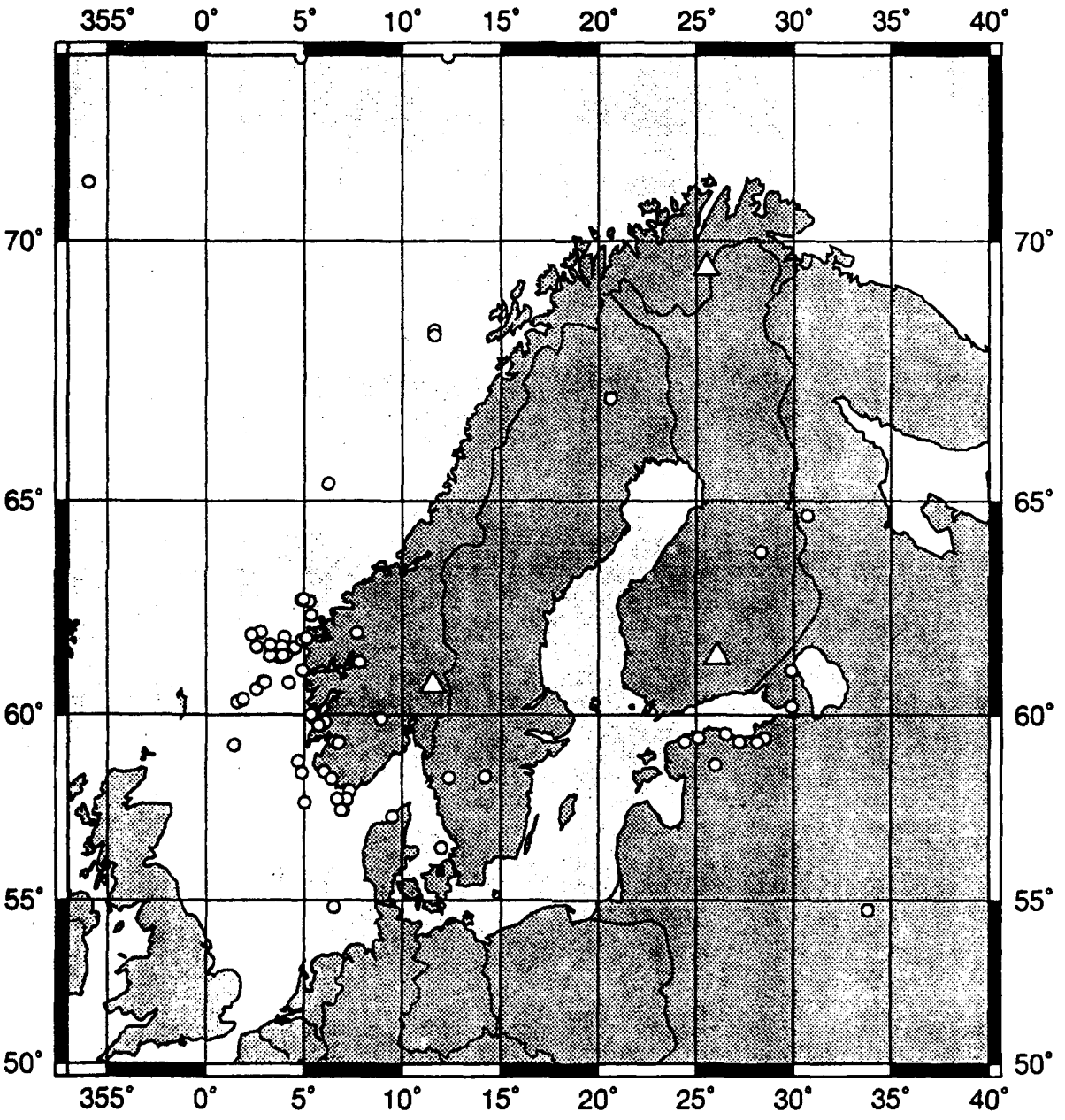

Figure 1. Locations of training events used in this study.

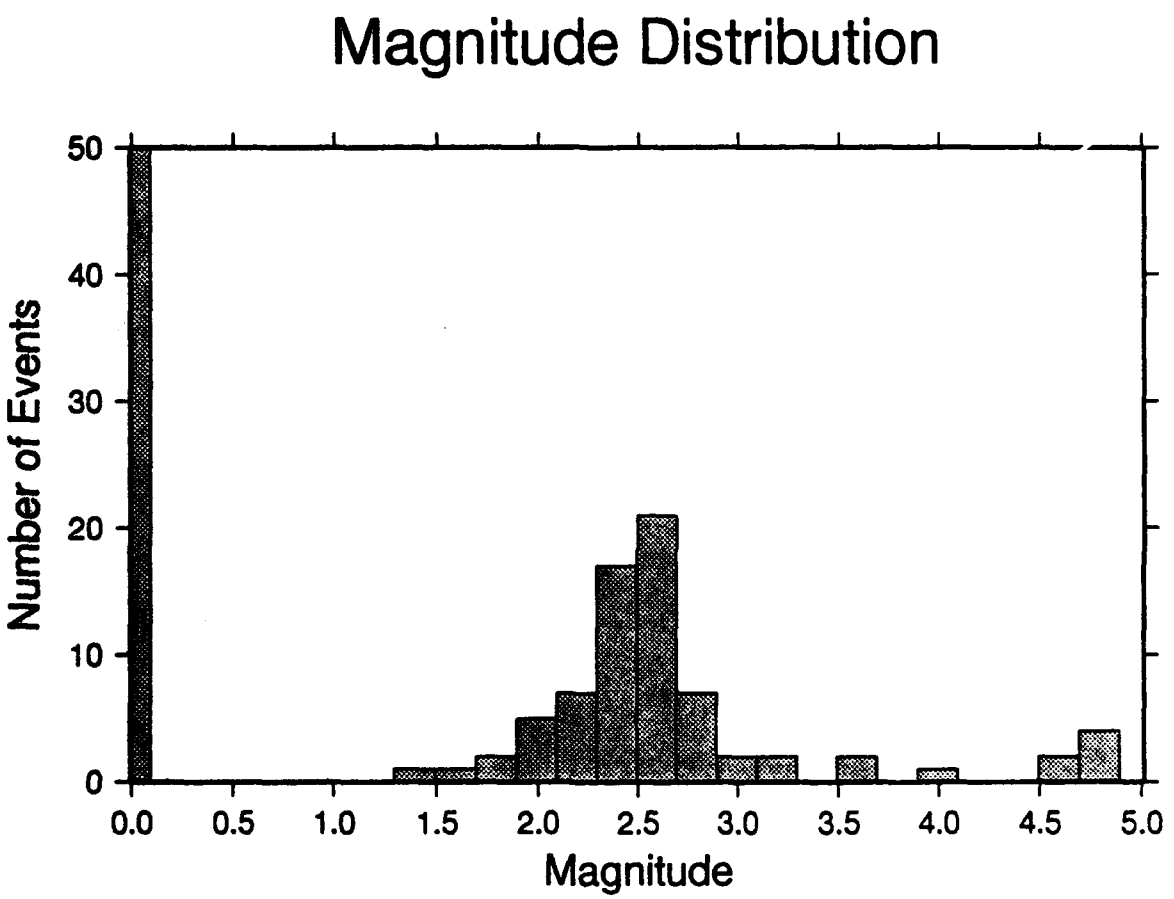

Figure 2. Magnitude distribution of events used in this study.

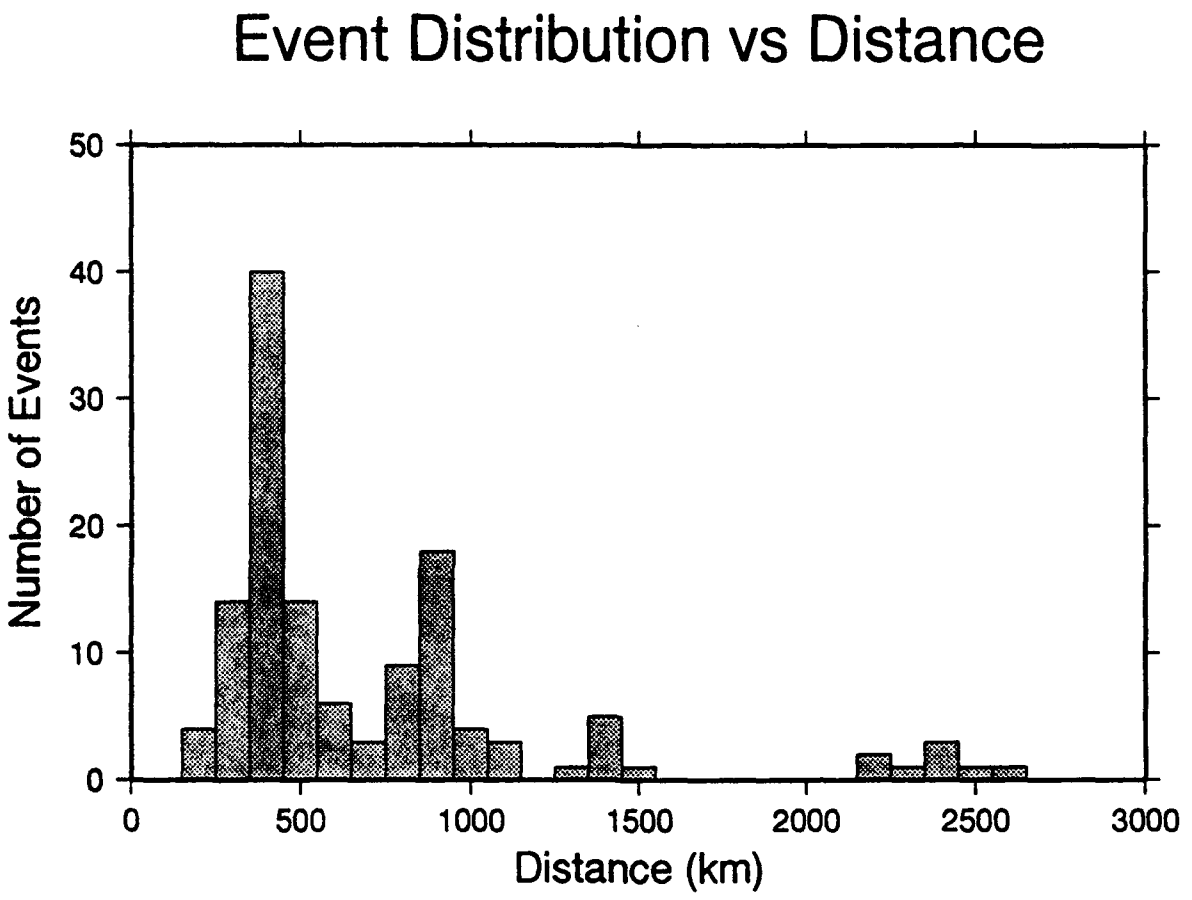

Figure 3. Distance distribution of events used in this study.

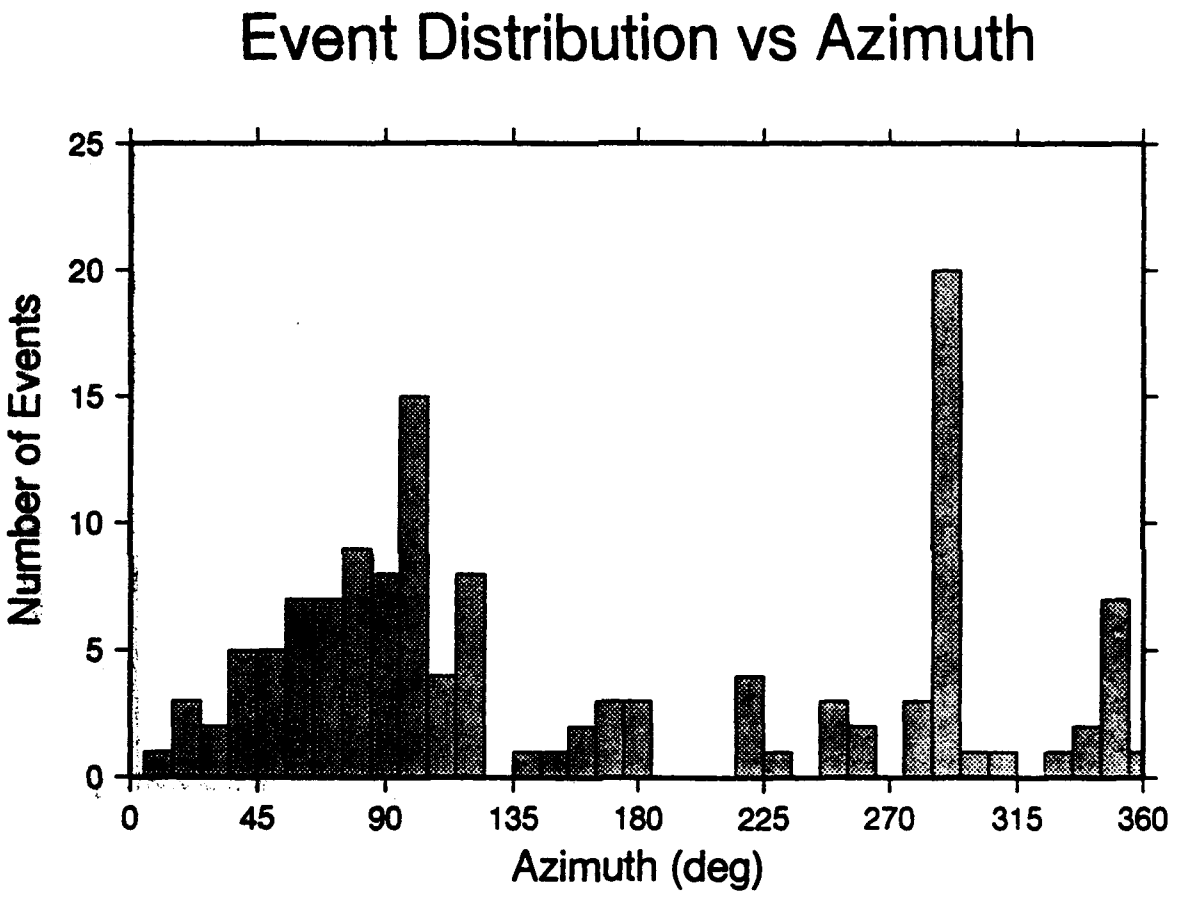

Figure 4. Azimuth distribution of events used in this study.

3. Signal Parameters and Analysis

3.1 Selection of Signal Parameters and Discriminants

The signal parameters chosen as inputs to the ANN's were based largely on the predicted characteristics of earthquake and explosion sources and were extracted to enhance class separability. These source characteristics and associated parameters are shown in *Table 2.*

Table 2. Extracted Signal Parameters

Signal Attribute	Source Characteristic	Parameter
Spectral modulation	Source multiplicity	Cepstral variance
High-frequency content	Source duration	Third moment of frequency
Amplitude ratios	Shear excitation	Pn/Sn, Pn/Lg
Peak frequency	Source extent	Centroid frequency
Amplitude distribution	Stochastic measure	Skewness, kurtosis

Amplitude ratios are extracted in a series of adjacent frequency bins and are also averaged across the entire signal band. The assemblage of training data also includes supplemental independent variables such as magnitude, distance, azimuth and signal processing attributes such as SNR as explicit input variables or as potential corrections to other measured quantities. These include categorical information as well (mine site, geographical region, etc.). In general the training set should retain all important spatial and temporal characteristics of the physical system that might aid in concept-testing, and assure that classifications are based solely on the source type. In a sense, this is an expert system component of the methodology that is a balance between approaches that use raw time series or spectral amplitudes as input and those that strictly apply rule or case-based reasoning schemes in the selection of input parameters. Various data transformations are used at the parameter extraction stage (e.g. log x) to reduce variance and render quadratic relations linear (e.g. geometric spreading, attenuation).

It is important to note at this point the constraints which discourage the use of time series or raw spectral amplitudes as input to the classification procedure. The dimensionality of the input training set together with the number of desired outputs (1-explosion, 2-earthquake), and hidden layer nodes determines the number of weighting coefficients which must be estimated. The number of coefficients is approximately equal to the number of training examples required for the even-determined problem. Given some level of noise in the data unrelated to source type, the number of required training examples is larger (Klimasauskas and

DuBose, 1991). In a supervised learning experiment the number of confidently identified events is generally limited to order 100. The use of even small waveform segments or binned spectral amplitudes results in network configurations with thousands of undetermined weighting coefficients. In addition, the task of interpreting the network solution in terms of physically meaningful source characteristics becomes exceedingly difficult.

Since the ANN classification problem is closely related to the more general problem of pattern recognition, it is classically confounded by variations due to translation, rotation, and scale. In the seismic source classification problem, these variations are not directly related to source type. Time series data regretably incorporate all of these as follows:

- Scale: Events with varying magnitudes and distance (requires correction for event size, geometric spreading, and anelastic attenuation).

- Translation: Events with varying phase spectra (requires correction for phase delays imposed by path and recording site).

- Rotation: Events recorded at varying azimuths and incidence angles (requires rotation of three-component data along direction of propagation).

The use of raw spectral amplitudes appears to eliminate variations due to translation but retains variations due to scale and rotation. Ideally, classification success would not depend on the confident determination of path and site effects which might not be available.

Guiding factors in the selection of parameters to extract from the data were the ultimate goals and constraints of the ANN classification procedure, i.e.

- To reduce the dimensionality of the input variables and determine their relative importance.

- To optimize the size of the ANN hidden layer configuration.

- To identify and explain outliers.

- To insure against classification based incorrectly on parameter measures not related to event type.

- To provide realistic performance measures in the form of probabilities of correct and incorrect classifications.

While accomplishing these goals it would also be advantageous to employ techniques that reveal functional relationships among the input parameters that can be tested against physical concepts or used to further reduce dimensionality.

Given these factors, the following specific signal parameters and discriminants were selected for extraction and inclusion in this study:

- Broadband P_n/S_n spectral ratio
- P_n/S_n spectral ratio (2-5 Hz)
- P_n/S_n spectral ratio (5-10 Hz)
- P_n/S_n spectral ratio (10-20 Hz)
- Broadband P_n/L_g spectral ratio
- P_n/L_g spectral ratio (2-5Hz)
- P_n/L_g spectral ratio (5-10 Hz)
- P_n/L_g spectral ratio (10-20 Hz)
- P_n cepstral variance
- S_n cepstral variance
- L_g cepstral variance
- P_n third moment of frequency (TMF)
- S_n TMF
- L_g TMF

3.2 Data Review and Parameter Extraction

Prior to parameter extraction, each channel of data is carefully reviewed prior to inclusion in the analysis. This review process is very important, since our methodology is based on the computation of spectral parameters derived from the waveform data. If there are any problems with the waveform data, these will be reflected in the derived spectral parameters, which will then make their way into the machine learning experiments. One then risks the possibility that the ANN's will *learn* artifacts of the data which are unrelated to any source physics. On some

of the recording from the NORESS array, spikes and data dropouts were an occasional occurrence. These bad waveform segments were eliminated from the analysis.

To extract the selected parameters, the waveforms were displayed on a Sun workstation in unfiltered, low pass filtered, and high pass filtered versions. The time windows of the P_n, S_n, and L_g waves were individually selected for each event. The selected signal parameters were then estimated from all of the vertical data channel using the method of the periodogram.

3.3 Analysis of Signal Parameters

The proper application of machine learning techniques such as ANN's depends to a large extent on an understanding of the data. Our methodology for exploring the data before ANN design and training is based on both a visual and statistical analysis of the data. The statistical analysis includes simple descriptive statistics, stepwise discriminant analysis, and Principal Components Analysis.

3.3.1 Visual Examination of the Parameter Database

Values for all of the extracted signal parameters are shown in *Figures 5-18*. For each plot, the horizontal axis corresponds to the event number. The events have been presorted into earthquake and explosion classes. Thus, the vertical line which apparently separates the two classes is not relevant in these plots. A linear discriminant function which separates the classes of events would be represented by a horizontal line in all cases. The vertical axis is simply the scaled value of each signal parameter, i.e. scaled to the range 0-1. Note that in some of the plots, there are parameter values that are exactly 0. These represent cases where a particular parameter measurement was not possible. For example, earthquakes located in the Greenland Sea to the northwest of NORESS do not produce visible L_g waves, due to the lack of L_g propagation in oceanic crust. Hence, parameters such as P_n/L_g spectral ratios cannot be made for these events.

A visual examination of these parameter plots points out some simple but important observations. First of all, no single parameter completely separates the data into earthquake and explosion classes. However, some parameters are better than others for class separability. Summarizing our visual examination, we find:

- Broadband P_n/S_n: Good class separation with few earthquake outliers. (*Figure 5*)

- P_n/S_n (2-5 Hz): Poor class separation. (*Figure 6*)

- P_n/S_n (5-10 Hz): Fair class separation with overlap. (*Figure 7*)

- P_n/S_n (10-20 Hz): Good class separation with few earthquake outliers. (*Figure 8*)

- Broadband P_n/L_g: Fair class separation with overlap. (*Figure 9*)

- P_n/L_g (2-5 Hz): Fair class separation with overlap. (*Figure 10*)

- P_n/L_g (5-10 Hz): Fair class separation with some overlap and outliers. (*Figure 11*)

- P_n/L_g (10-20 Hz): Fair class separation with some overlap and one outlier. (*Figure 12*)

- P_n cepstral variance: Poor class separation. (*Figure 13*)

- S_n cepstral variance: Fair class separation with some overlap. (*Figure 14*)

- L_g cepstral variance: Fair class separation with some overlap. (*Figure 15*)

- P_n TMF: Poor class separation. (*Figure 16*)

- S_n TMF: Poor class separation. (*Figure 17*)

- L_g TMF: Poor class separation. (*Figure 18*)

3.3.2 Descriptive Statistics

Descriptive statistics of a multidimensional dataspace includes means and variances of each parameter, plus the crosscorrelation of all parameters. In the figures which accompany this section, the parameters are indicated by number rather than name, and the ordering of the parameters is somewhat different than that presented earlier. The parameters and their index number are:

1 Broadband Pn/Lg spectral ratio

2 Broadband Pn/Sn spectral ratio

3 Mean cepstral variance of Pn, Sn, and Lg

4 Pn/Lg spectral ratio, 2-5 Hz

5 Pn/Sn spectral ratio, 2-5 Hz

6 Pn/Lg spectral ratio, 5-10 Hz

7 Pn/Sn spectral ratio, 5-10 Hz

8 Pn/Lg spectral ratio, 10-20 Hz

9 Pn/Sn spectral ratio, 10-20 Hz

10 TMF of Pn

11 TMF of Sn

12 TMF of Lg

The difference in means for each parameter for the two classes, shown in *Figure 19*, points to parameters which provide good class separability. *Figure 19* shows that parameters 2 (broadband P_n/S_n spectral ratio), 3 (mean cepstral variance of P_n, S_n, and L_g), 6 (P_n/L_g spectral ratio from 5-10 Hz), and 7 (P_n/S_n spectral ratio from 5-10 Hz) provide the best class separability in the dataset.

The variance of each parameter for the two classes is shown in *Figure 20*. For each parameter, the plot shows that the variance for the earthquake class is significantly larger than the variance for the explosion class.

The crosscorrelation calculation (*Figure 21*) shows a strong correlation of certain parameters such as the P_n/L_g and P_n/S_n broadband spectral ratios, the broadband P_n/L_g and narrowband P_n/L_g (2-5 Hz) spectral ratios. Parameters with low correlation are the cepstral variances and spectral ratios (expected, since they measure different characteristics). The strong correlation of all TMF measures with distance renders these parameters useless for classification, unless a known path correction is applied to the parameters.

Stepwise discriminant analysis (Enslein et al., 1977) is a valuable tool in identifying the strong discriminant and discriminant pairs that successfully separate the majority of training events. It provides a means to reduce the number of input variables in a systematic fashion, while monitoring the generality of the linear model. As a byproduct of this procedure, the input variables are prioritized, and metrics are computed that aid in the design of the ANN. The stepwise discriminant analysis (*Figure 22*) shows that the six most important parameters in our dataset are numbers 6, 3, 2, 4, 5, and 8.

3.3.3 Principal Components Analysis

Principal Components Analysis (PCA) is a simple technique which seeks to describe the variance and covariance structure contained in an assemblage of data examples characterized by the same set of parameters. The technique is documented in many references (e.g. Enslien et al., 1977 and Jackson, 1991). Used here, it is essentially a traditional eigenvalue analysis applied to the covariance matrix of extracted parameters. The method as it was applied to the training set is described in the following five steps:

> **Step 1.** Form the data matrix of parameters (number of training examples by number of extracted parameters).
>
> **Step 2.** Operate on the columns by subtracting the mean and normalizing to a standard deviation of 1 (this step removes any *a priori* weighting of the parameters due to differences in units or number magnitude).
>
> **Step 3.** Form the covariance matrix from the normalized data matrix.
>
> **Step 4.** Perform a singular value decomposition (SVD) of the covariance matrix to obtain the ordered eigenvalues and associated eigenvectors.
>
> **Step 5.** Generate the *SCREE* plot to graphically select the number of significant principal components or equivalently, the portion of the total variance to retain. In a *SCREE* plots, one plots all of the characteristic roots of the covariance matrix, the values of the roots themselves being the ordinate and the root number the abscissa. (The term *SCREE* refers to the rubble at the bottom of a cliff. It was first applied to statistical analyses by Cattell, 1966.)

Step 5 is motivated by the desire to include a portion of the variance which supports the generality of the model by excluding variation due to noise. This preliminary PCA was applied to the entire set of extracted parameters although subsequent analyses will be applied separately to the explosion and earthquake populations.

PCA was applied to the training database compiled during this reporting period. A total of 12 parameters were used as inputs. The SCREE plot for this dataset is shown in *Figure 11.* Note the dominance of the first three principal components in this analysis. The cumulative percentage of the total variance of the principal components is shown in *Figure 12.* Here it is seen that the first three principal components account for more than 85% of the variance in the training database.

The results of the PCA and their impact so far on the ANN design can be summarized as follows:

1. The analysis shows that 3 hidden-nodes in a fully-connected backpropagation neural network should be sufficient to account for 86% of the data variance. The subsequent analysis by population could increase the requirement by a factor of 2 for a network with reduced connectivity.

2. This results in a maximum of $12 \times 3 + 3 \times 2 = 42$ network connections.

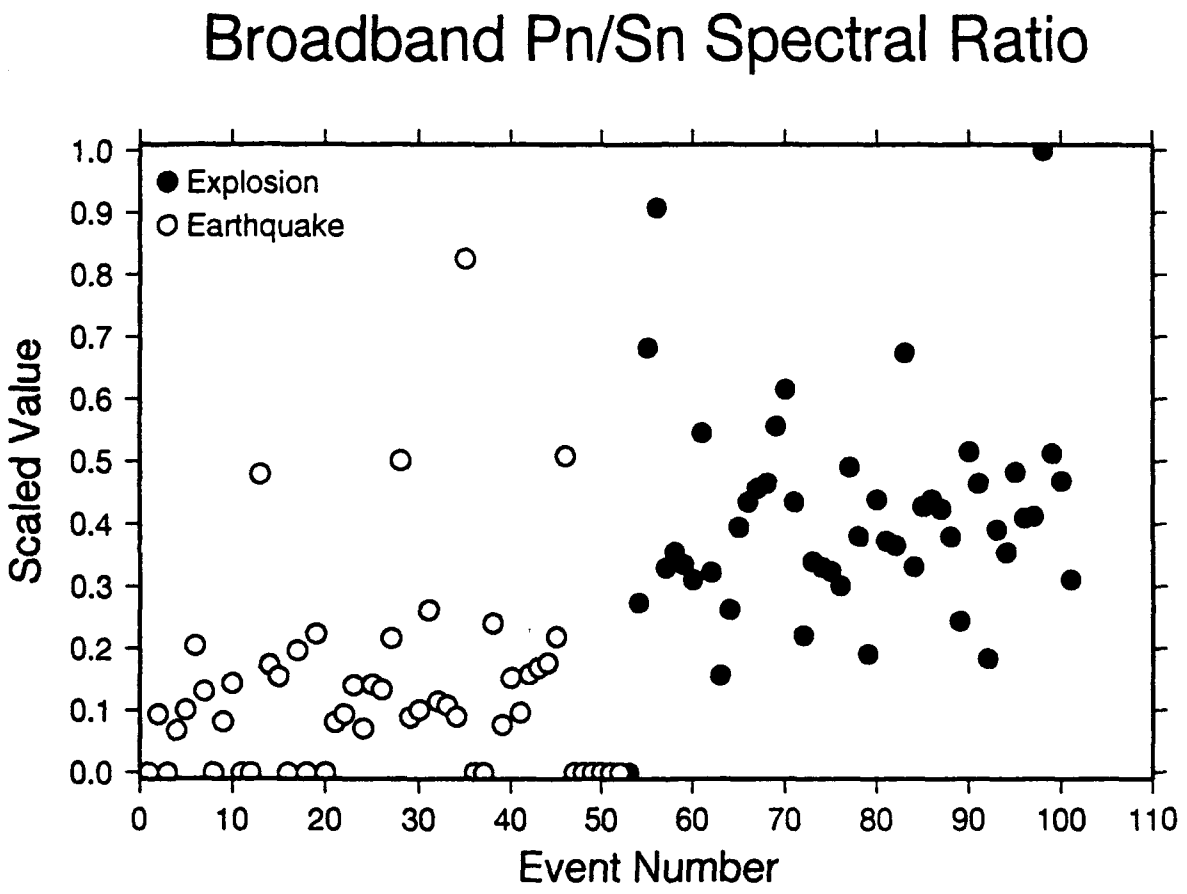

Figure 5. Broadband P_n/S_n spectral ratio for the dataset.

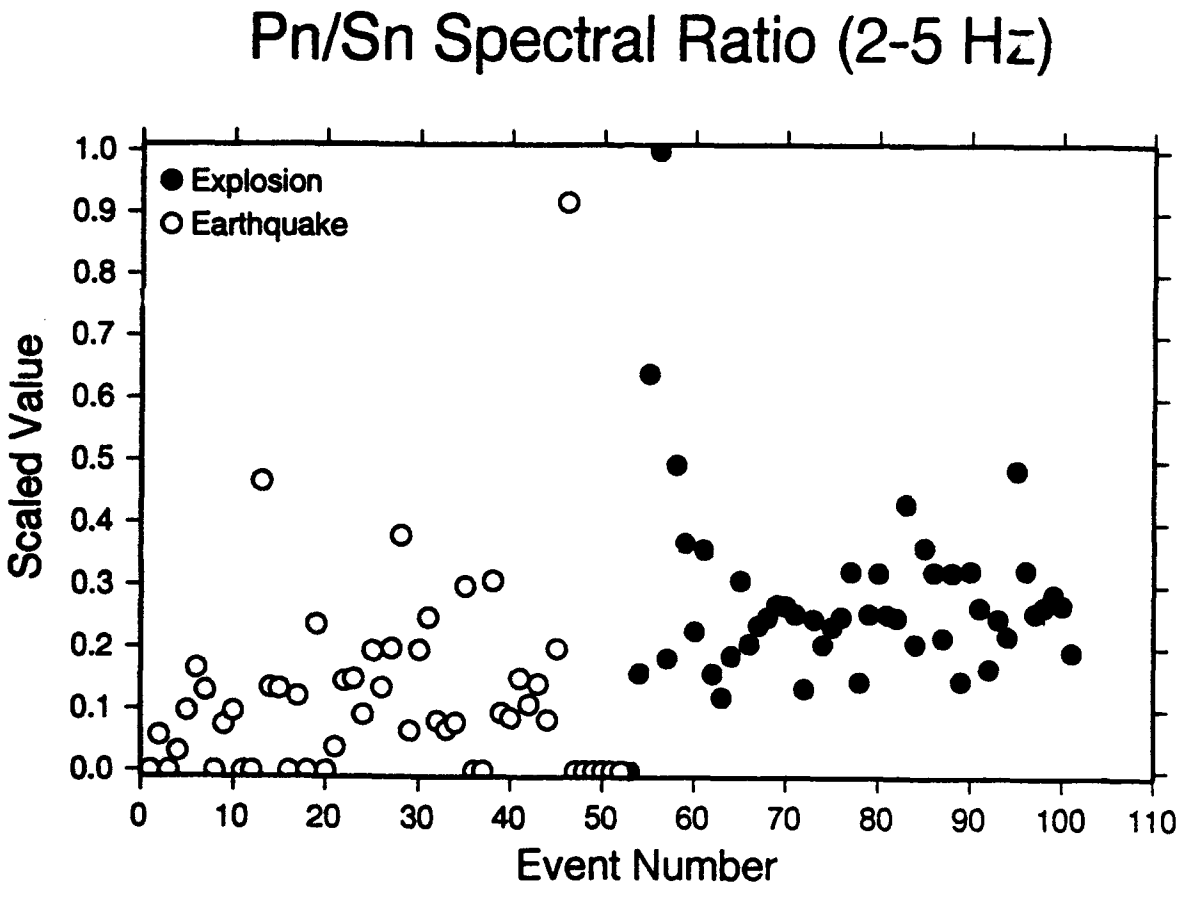

Figure 6. P_n/S_n spectral ratio from 2-5 Hz for the dataset.

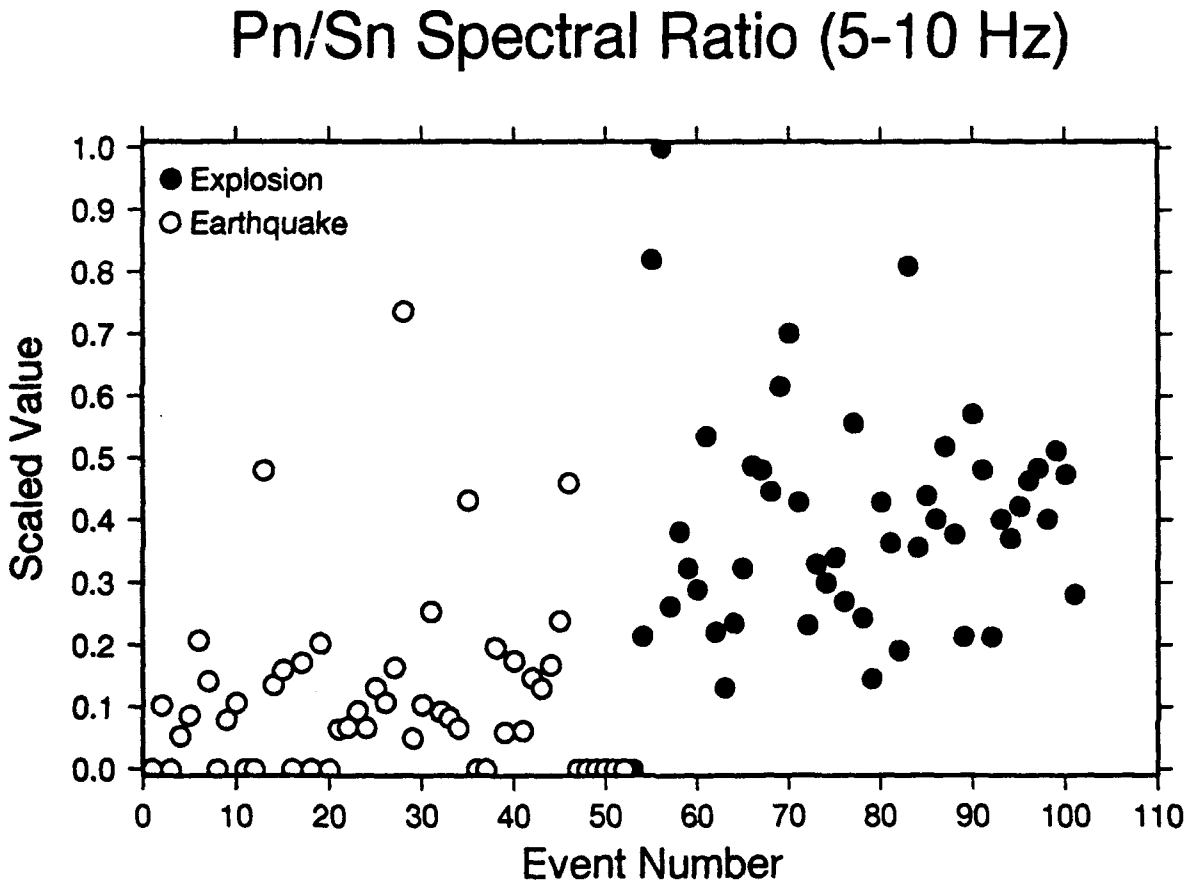

Figure 7. P_n/S_n spectral ratio from 5-10 Hz for the dataset.

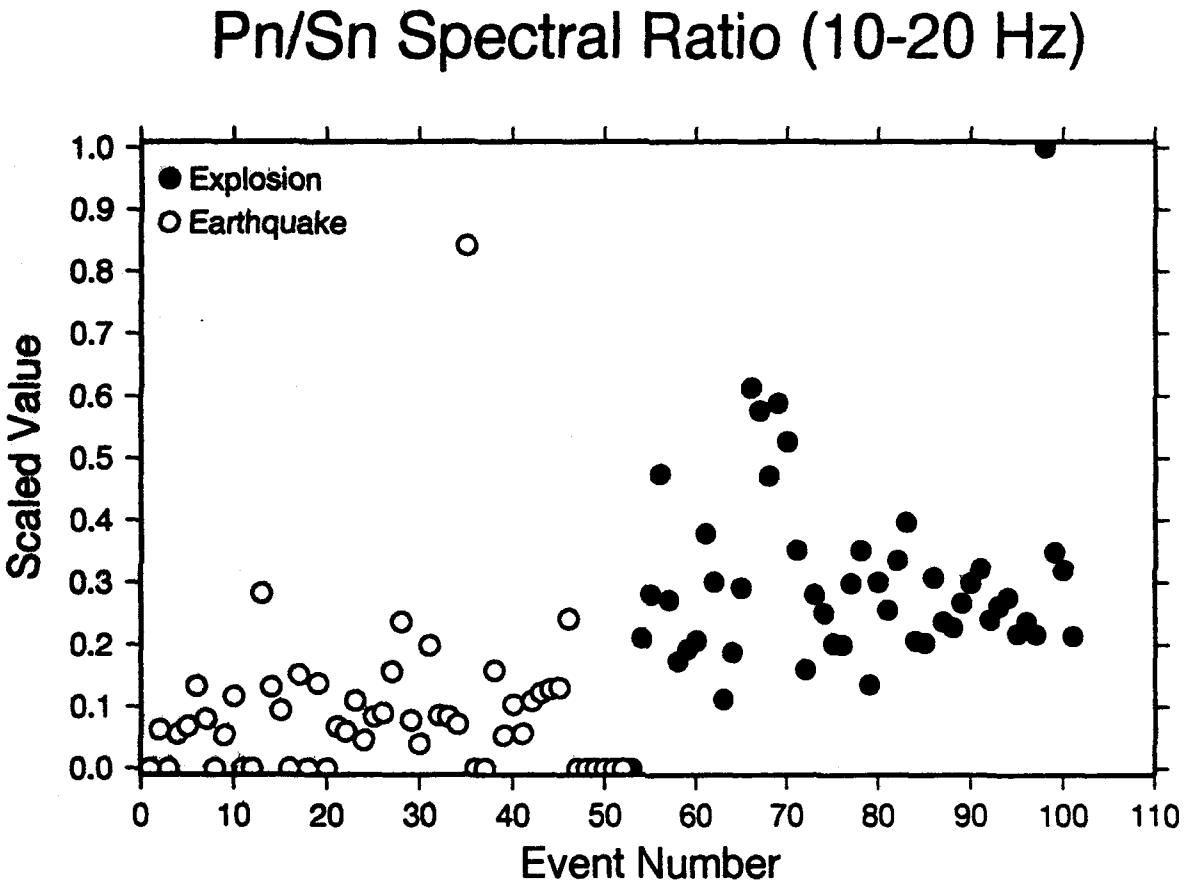

Figure 8. P_n/S_n spectral ratio from 10-20 Hz for the dataset.

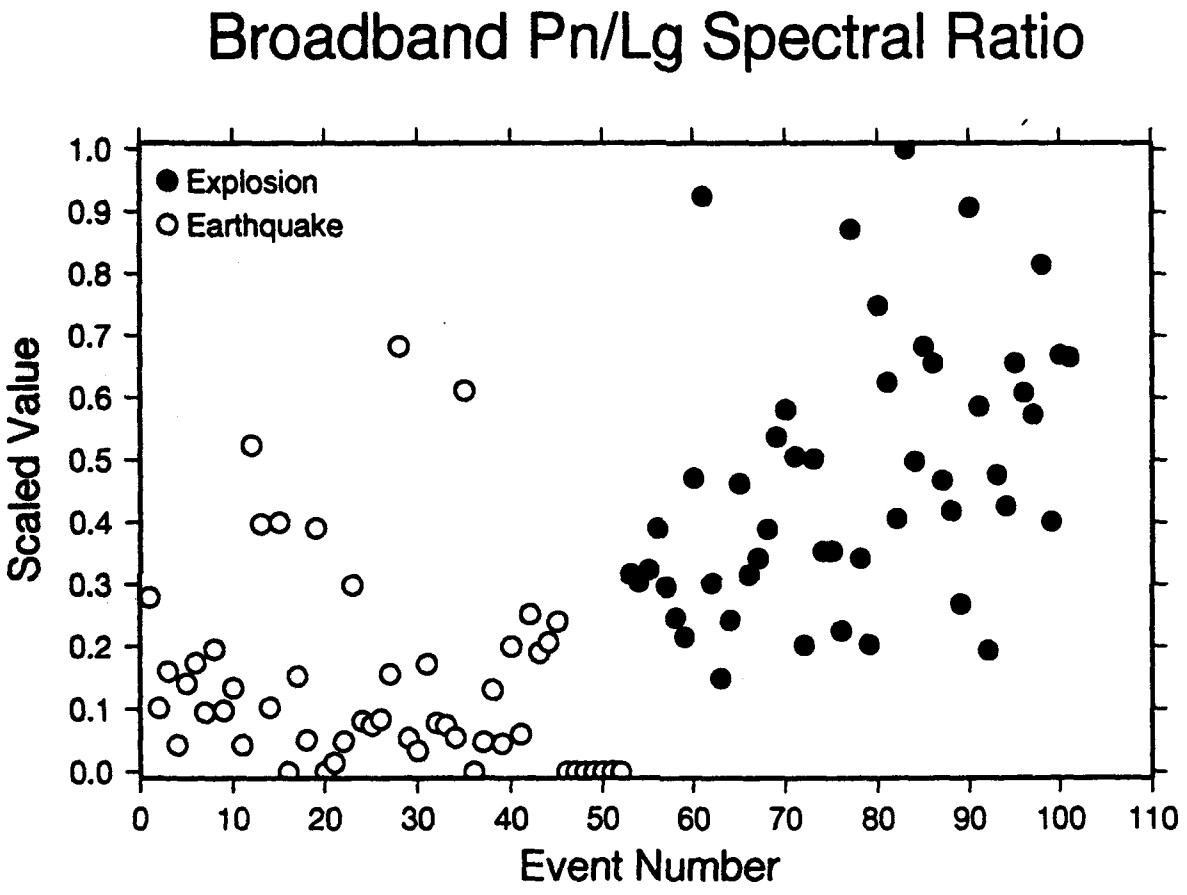

Figure 9. Broadband P_n/L_g spectral ratio for the dataset.

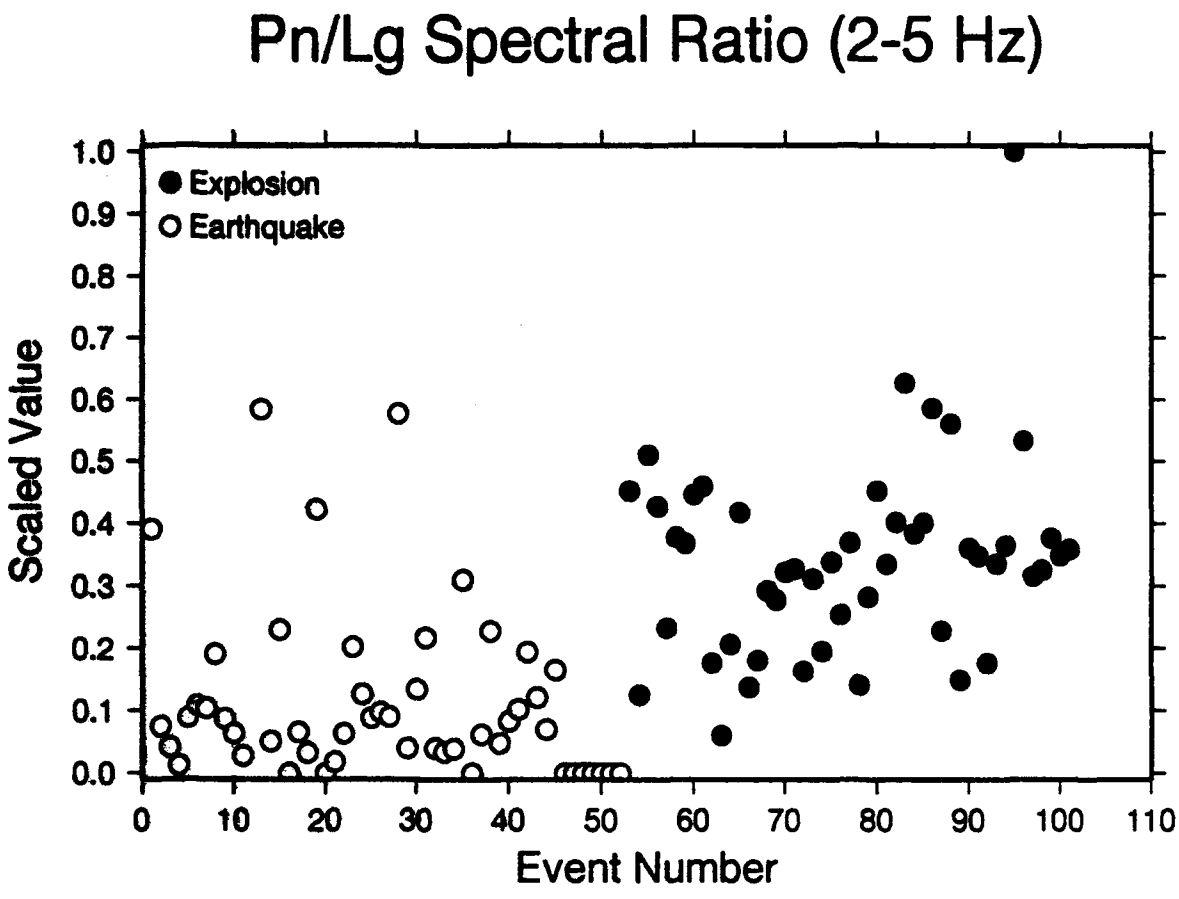

Figure 10. P_n/L_g spectral ratio from 2-5 Hz for the dataset.

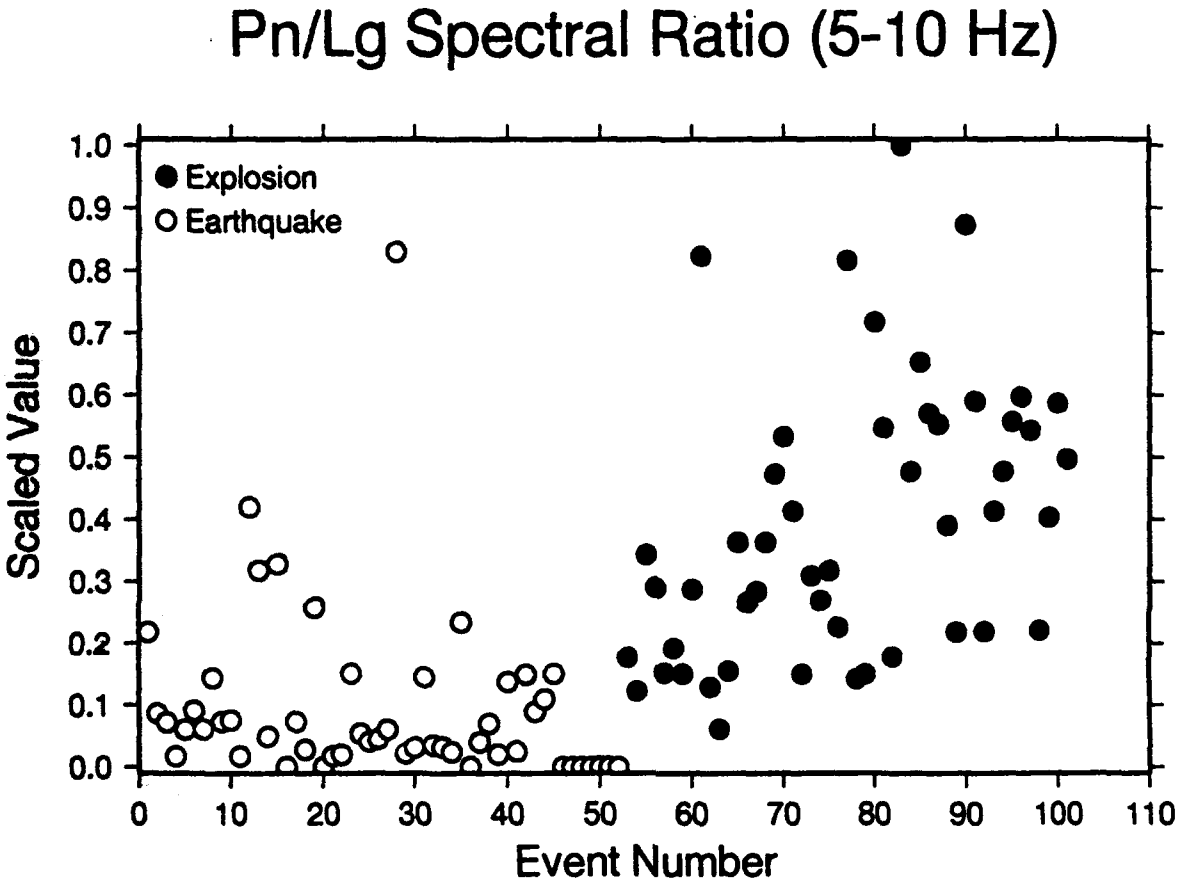

Figure 11. P_n/L_g spectral ratio from 5-10 Hz for the dataset.

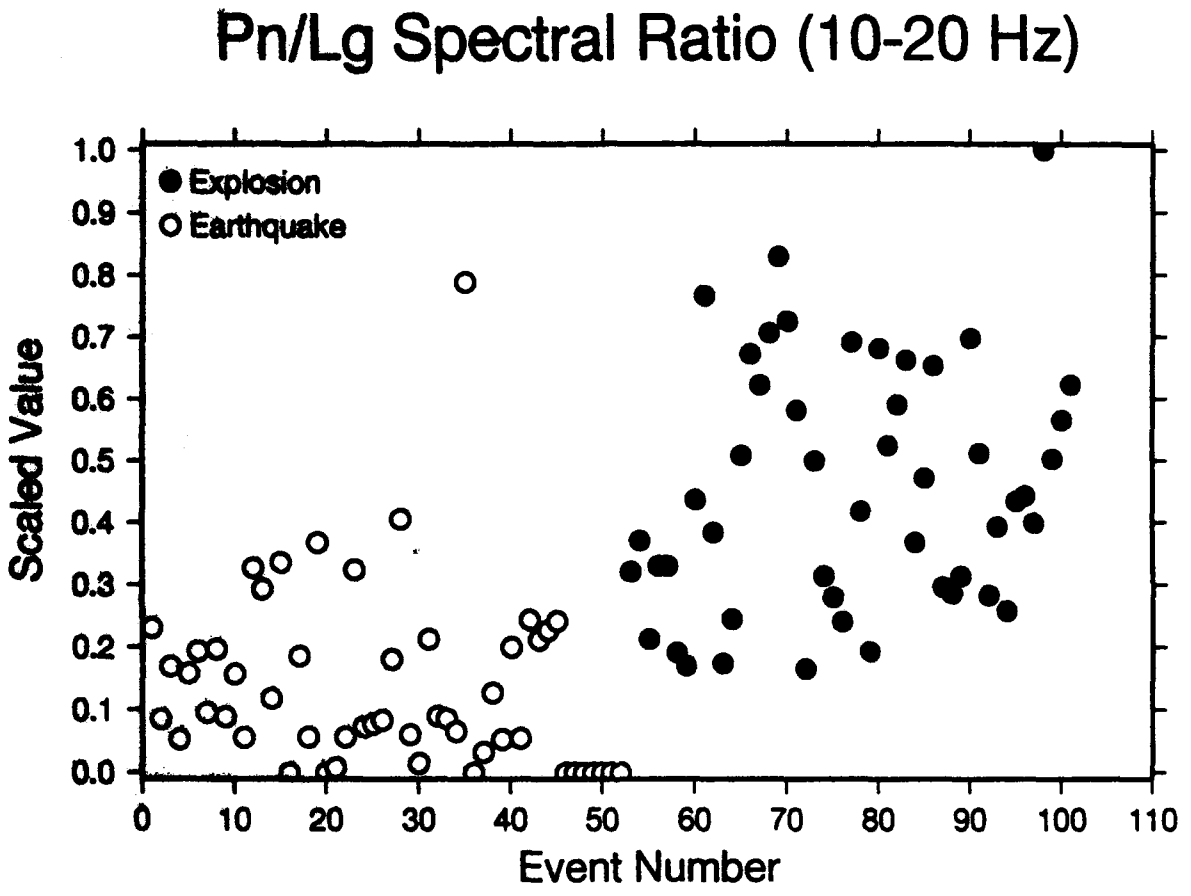

Figure 12. P_n/L_g spectral ratio from 10-20 Hz for the dataset.

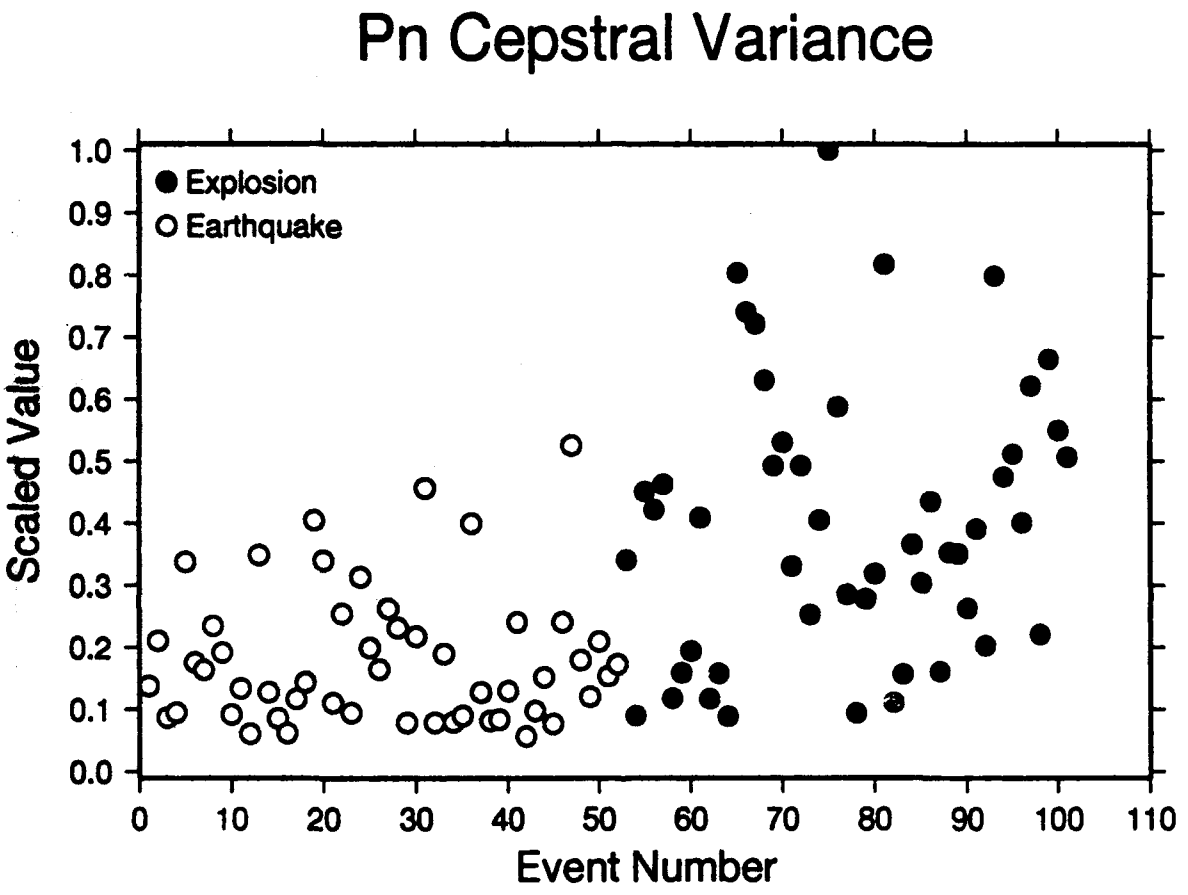

Figure 13. P_n cepstral variance for the dataset.

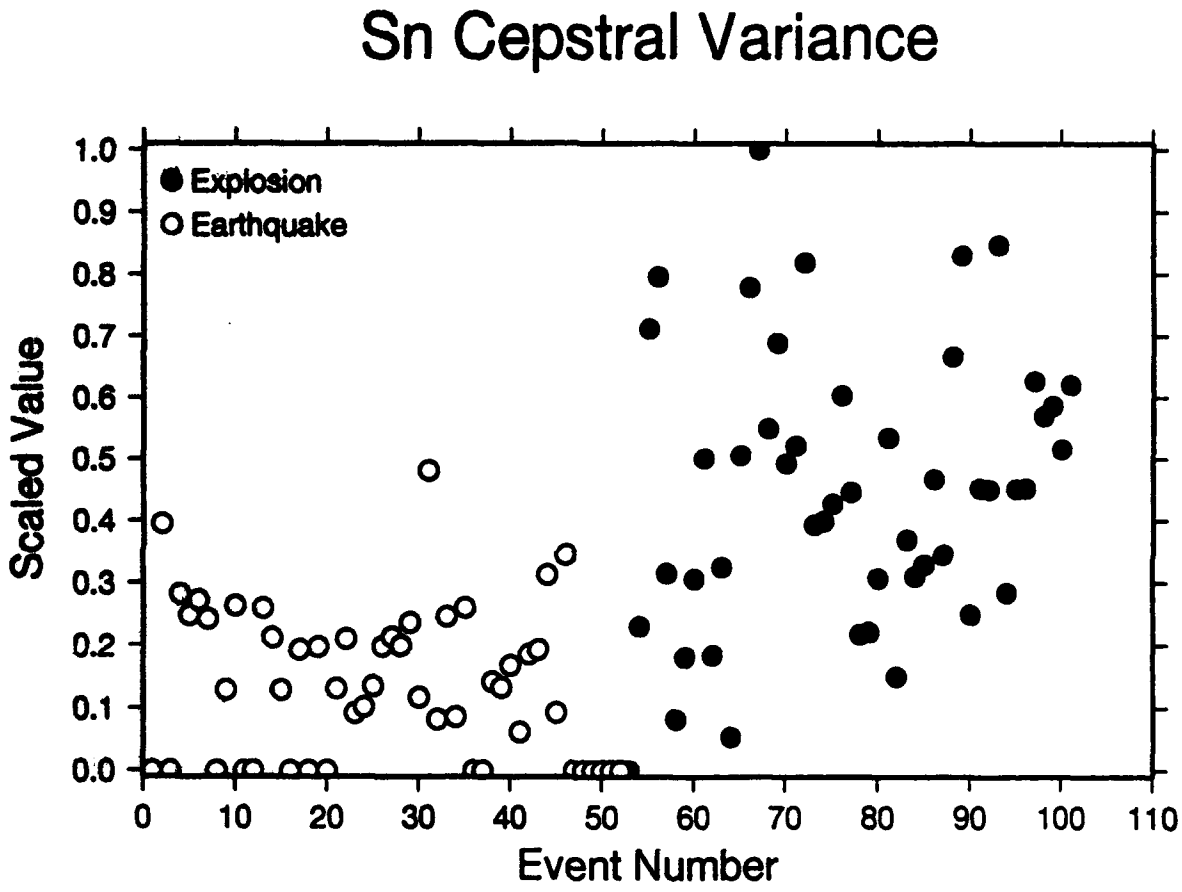

Figure 14. S_n cepstral variance for the dataset.

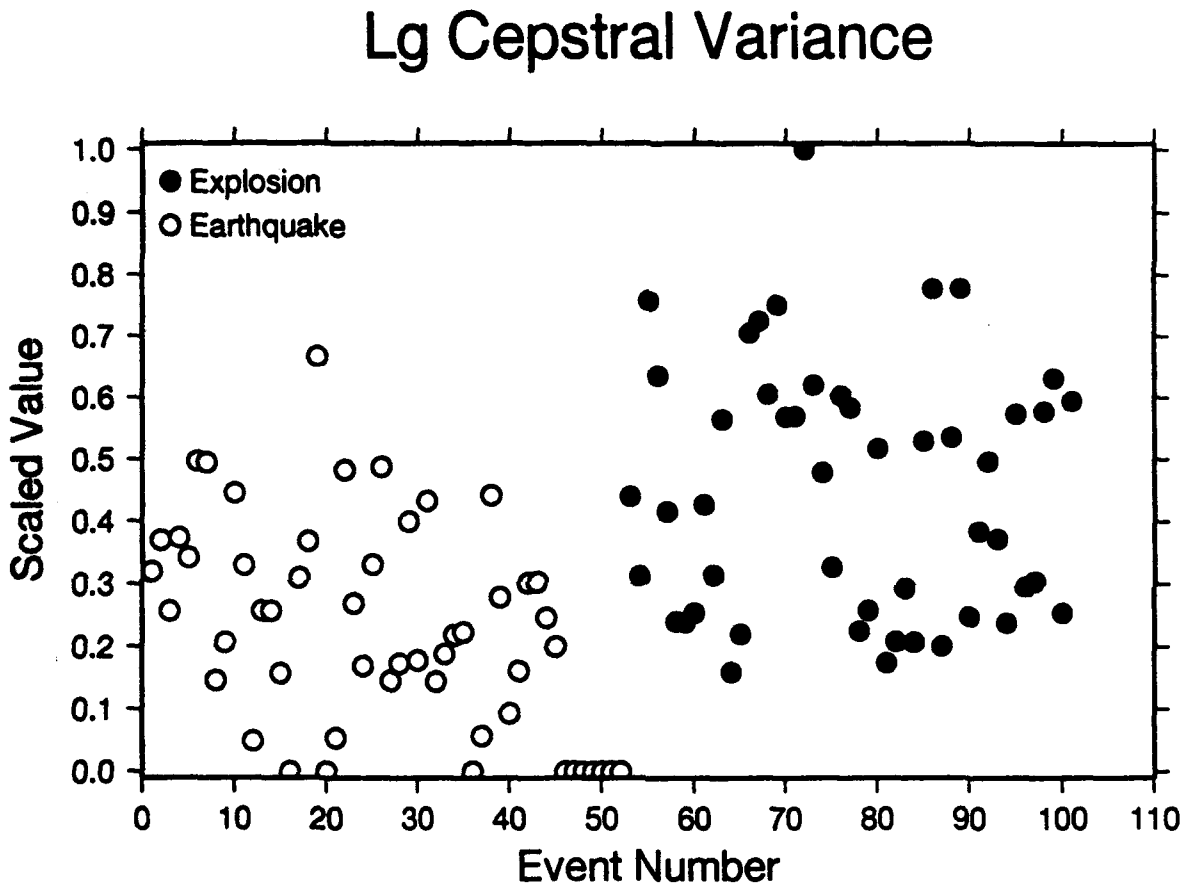

Figure 15. L_g cepstral variance for the dataset.

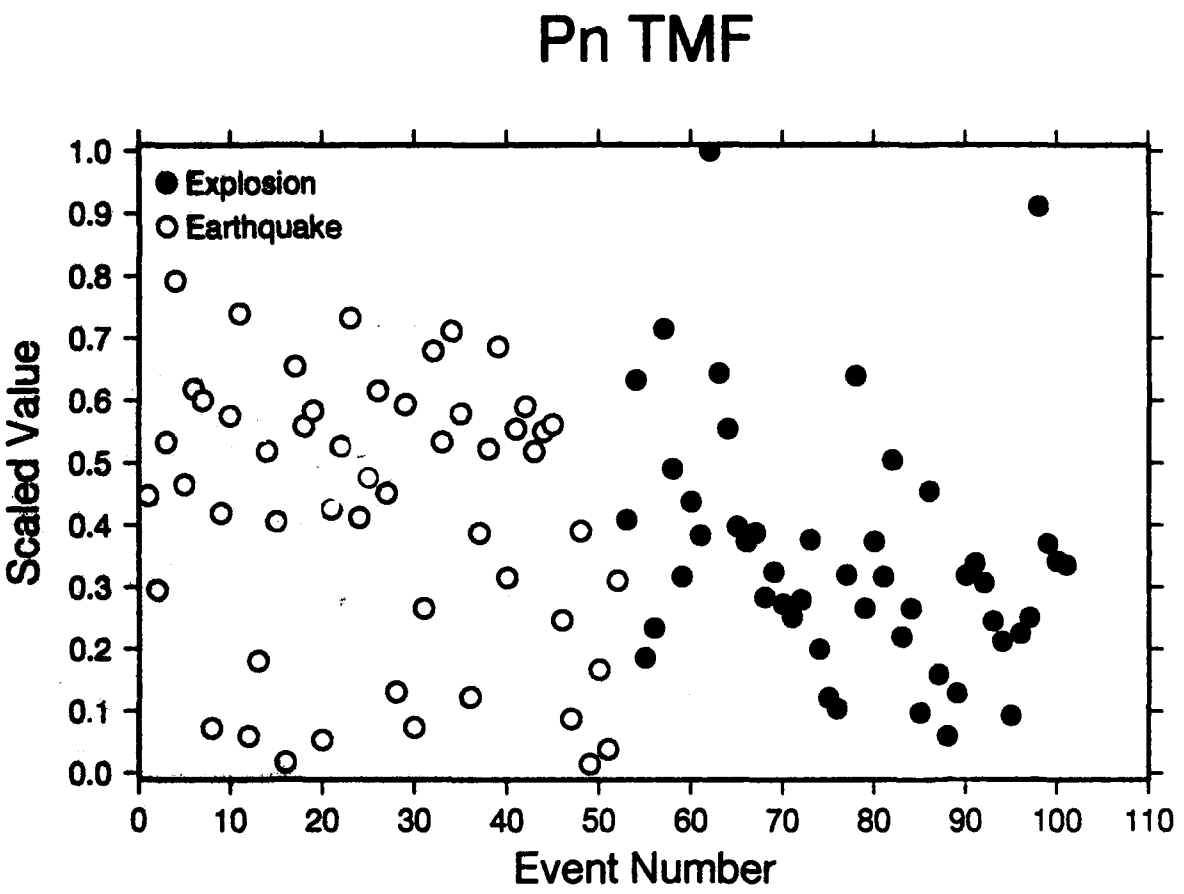

Figure 16. P_n TMF for the dataset.

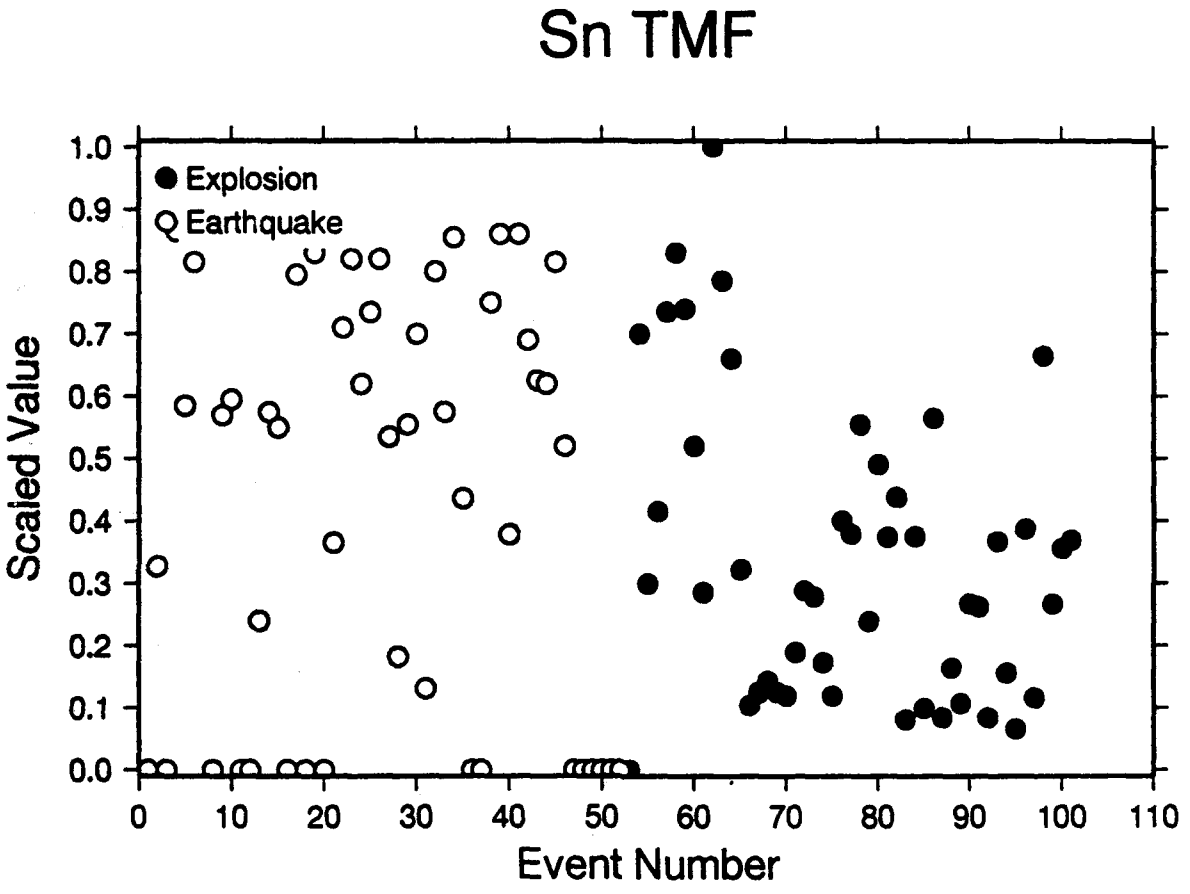

Figure 17. S_n TMF for the dataset.

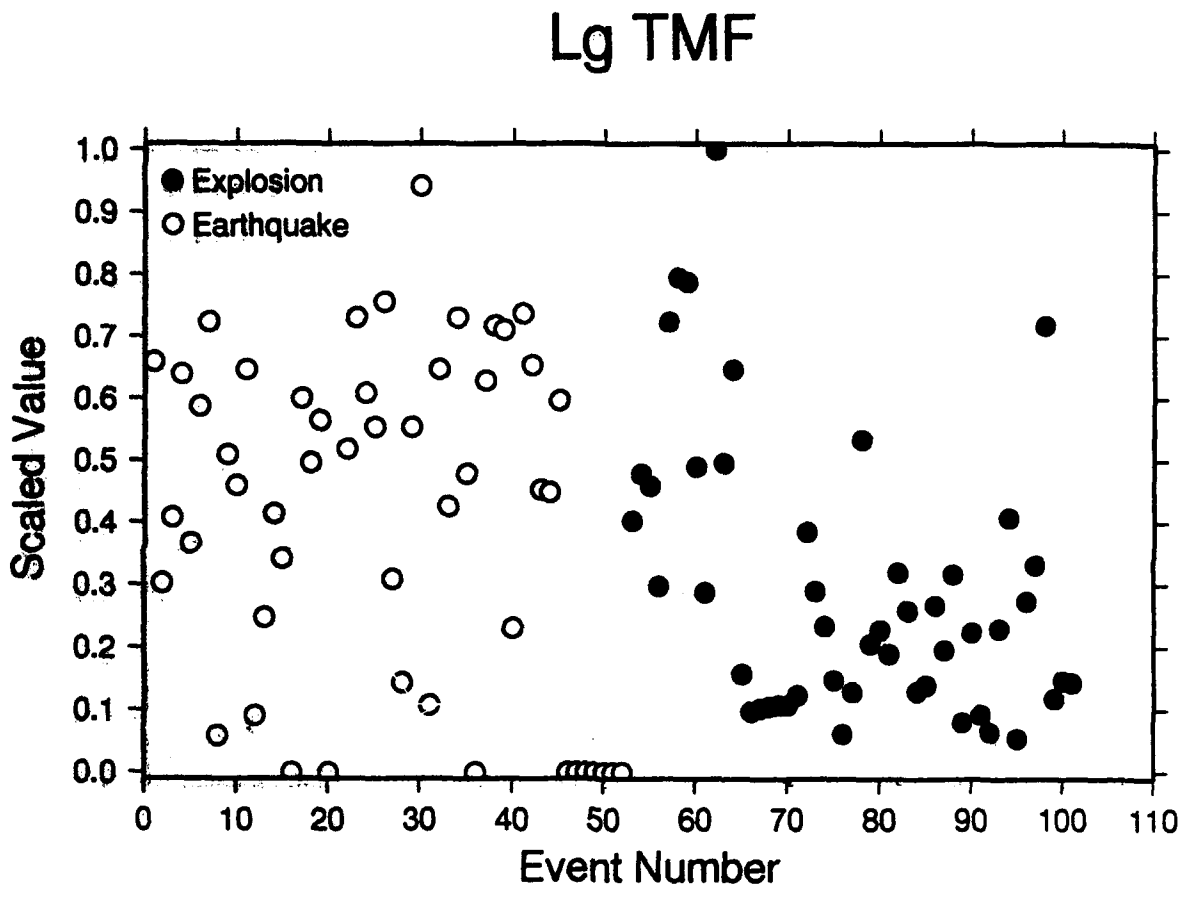

Figure 18. L_g TMF for the dataset.

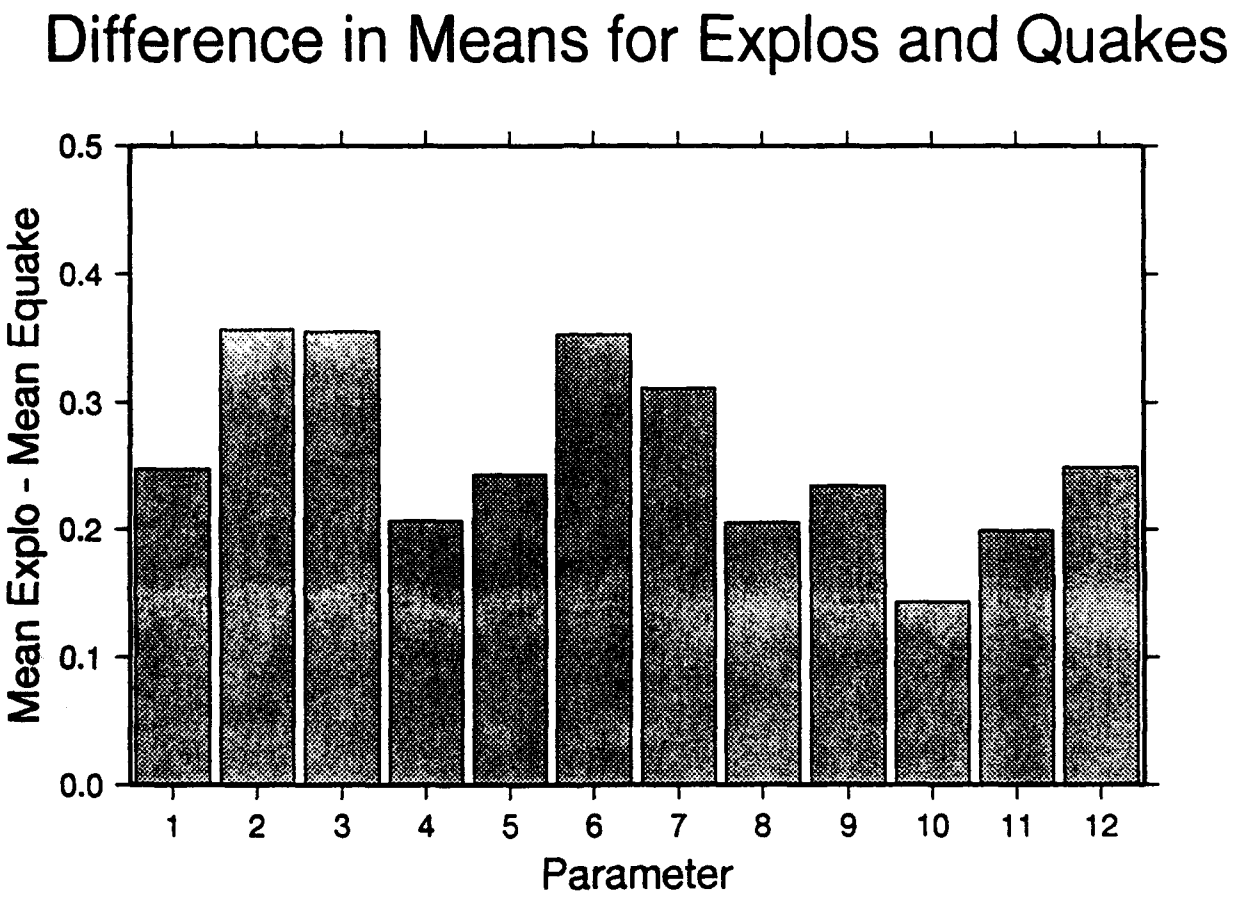

Figure 19. Difference in scaled means between the earthquake and explosion datasets.

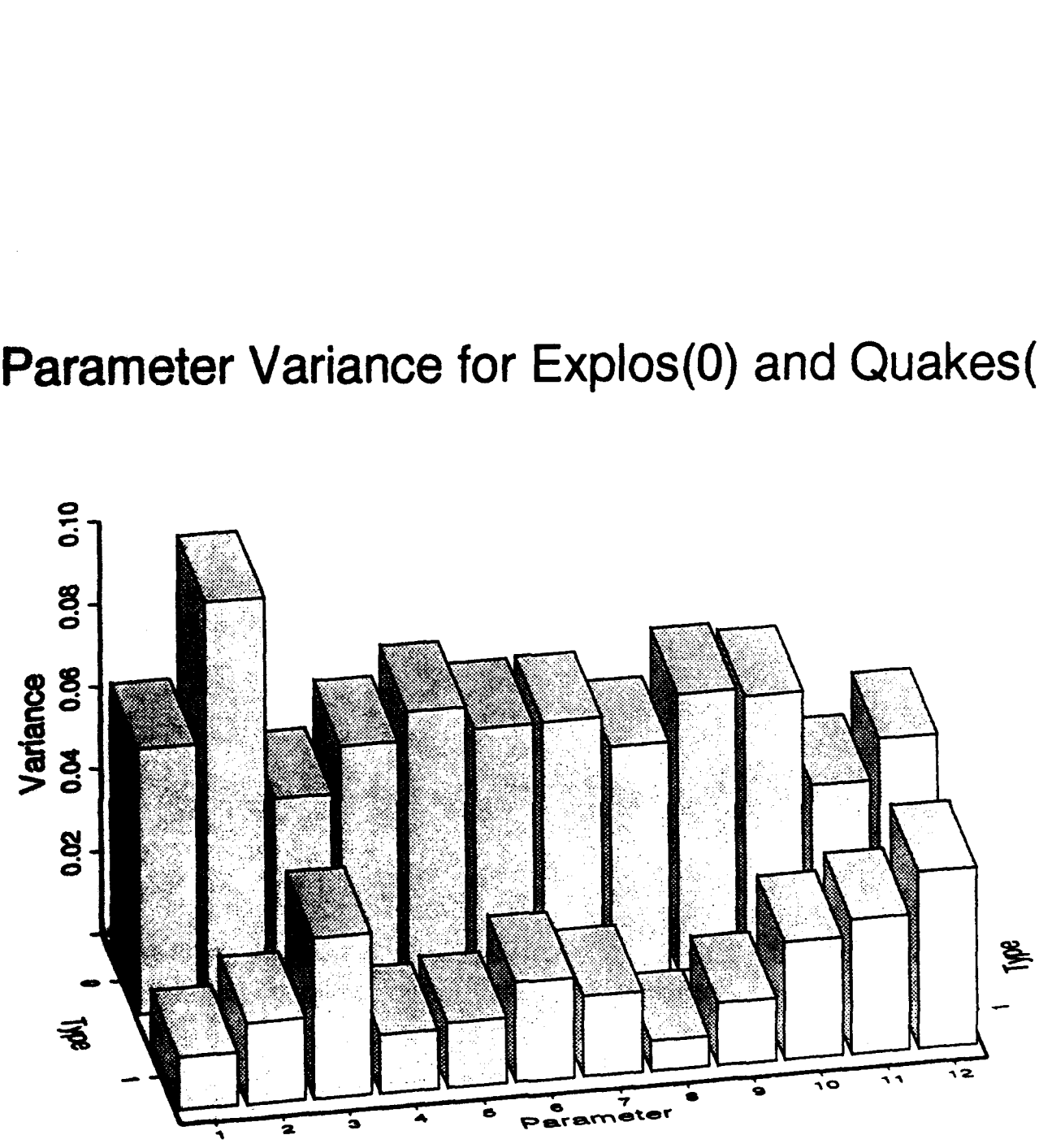

Figure 20. Variance for each signal parameter for the earthquake and explosion datasets.

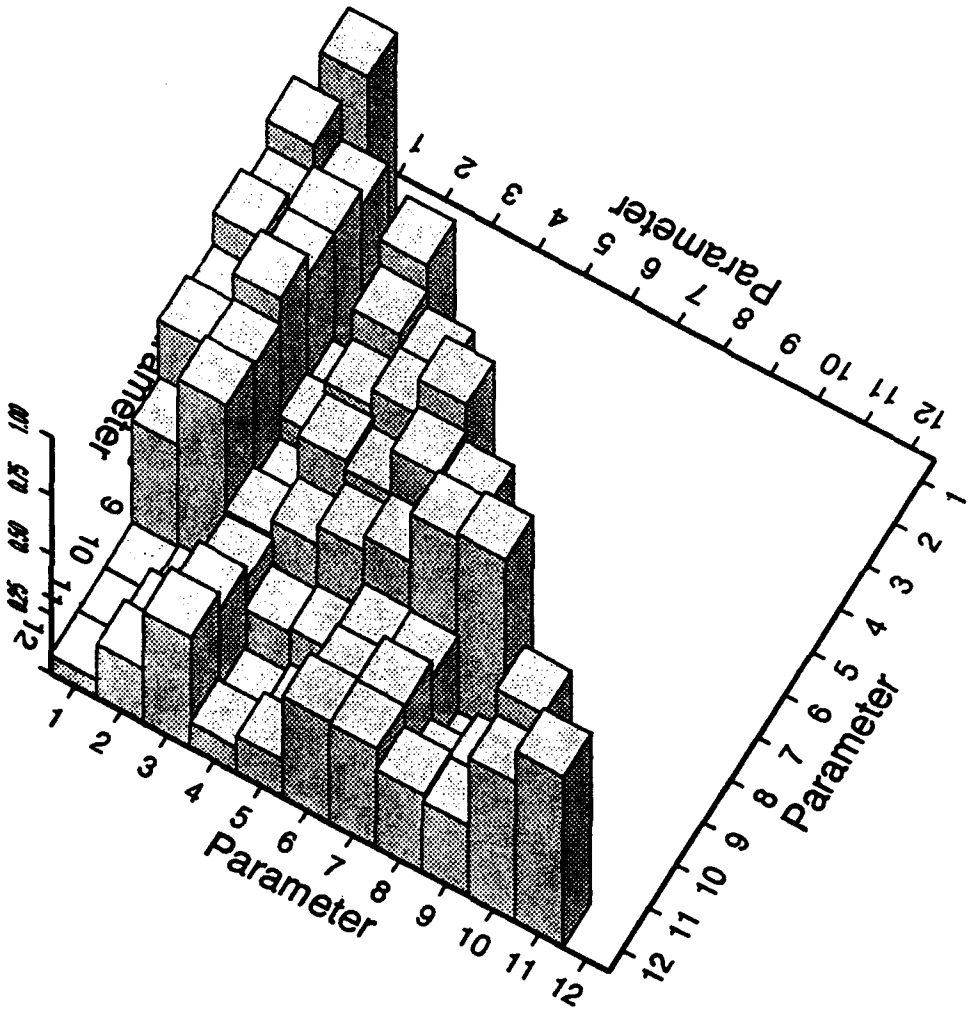

Figure 21. Crosscorrelation matrix for the signal parameters.

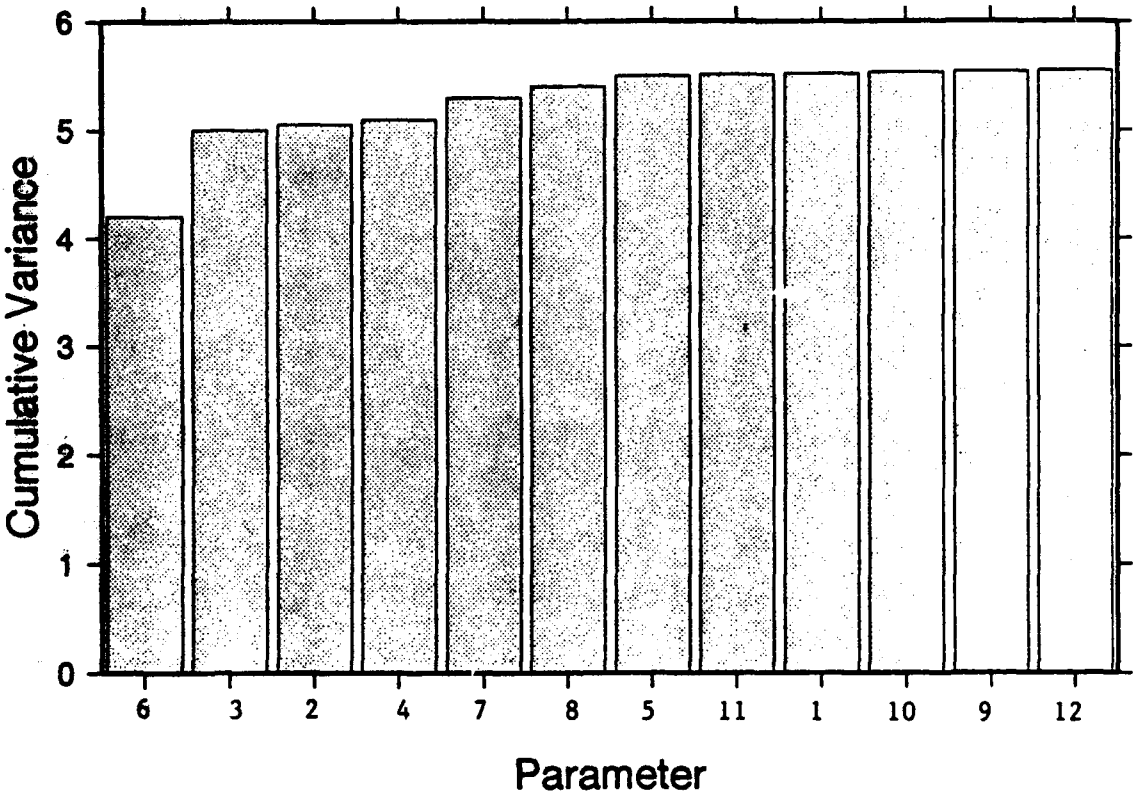

Figure 22. Stepwise discriminant analysis for the parameter dataset.

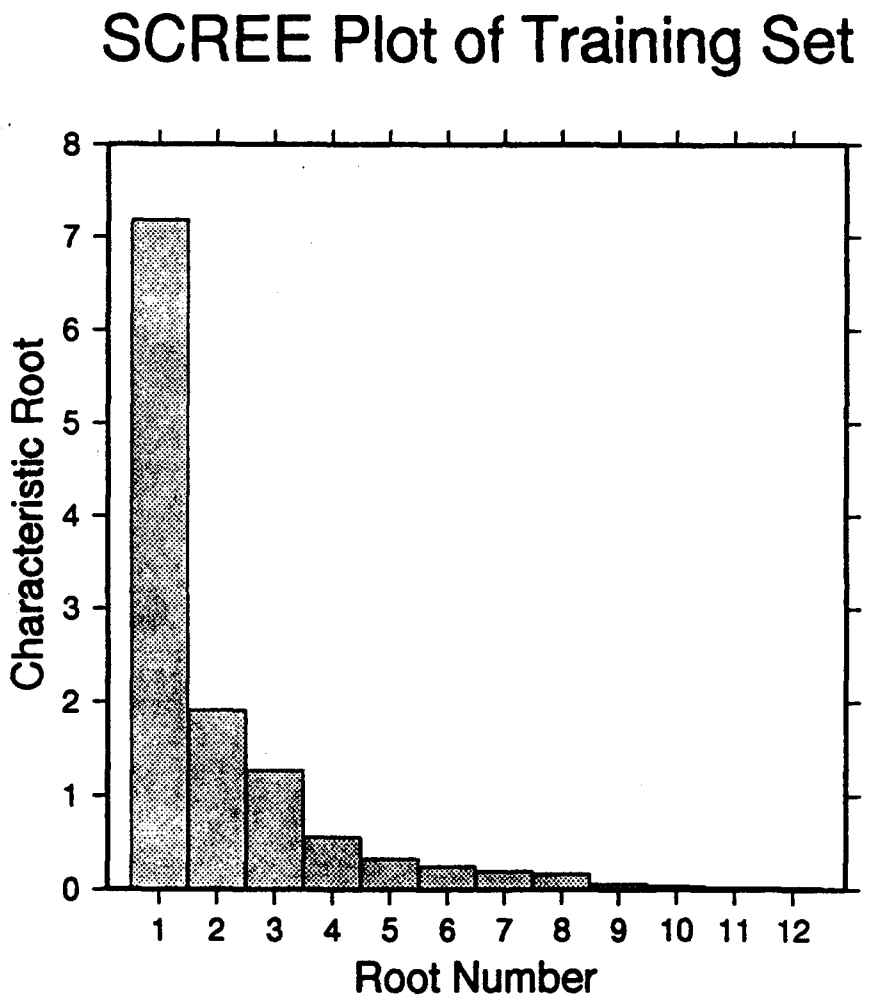

Figure 23. SCREE plot showing the size of the characteristic root vs. root number.

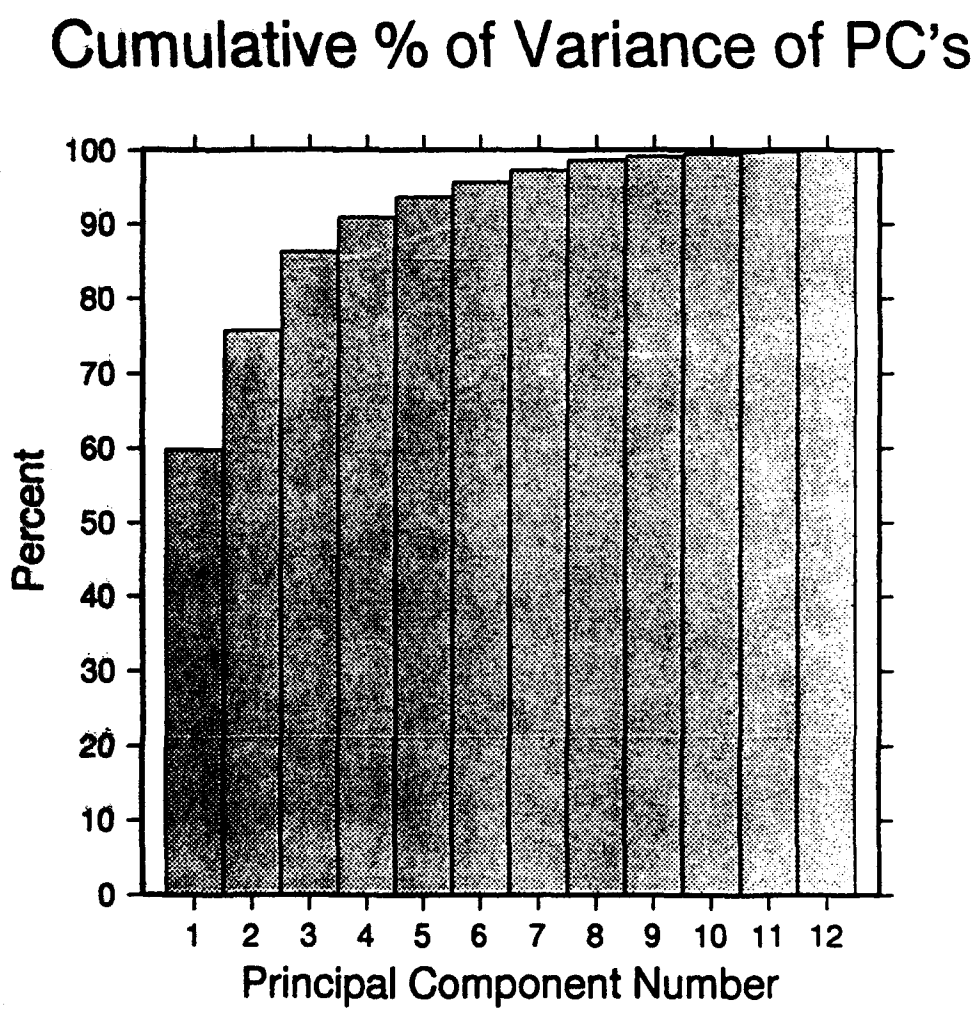

Figure 24. **Cumulative percent of the variation of the principal components.**

4. Neural Network Analysis

4.1 Neural Network Architecture and Training

There are many different types of artificial neural networks which can be applied to classification problems. For our experiments, we have chosen the fully connected backpropagation neural network. This simple network architecture is perfectly suited to supervised learning experiments. (Readers not familiar with neural networks or the neural network terminology used in this report can find the appropriate background material in the paper by Lippman, 1987.)

Many different experiments were performed with the ANN's, including variations on the number of inputs, number of outputs, and number of nodes in the hidden layer. For all of the experiments, a single hidden layer was used.

The final ANN design used in this study is shown in *Figure 25.* The network uses 10 inputs, a hidden layer with 3 nodes, and an output with 1 node. At each node, the nonlinear transfer function used was the arctangent function. This function ranges in value from -1 to +1. During supervised training, the explosions were assigned a value of +0.8, while the earthquakes were assigned a value of -0.8. After each training experiment, an RMS error of the classification fit was calculated. If the absolute value of the output classification of any event was determined to be less than this RMS error, then the event was classified as *unknown*.

The amount of time required to train an ANN will vary as a function of the number of training examples, the number of parameters per example, the ANN architecture, the computing resources, and the software used for the ANN. All of the examples described here were run on a Sun Sparcstation 2 with the NeuralWorks Professional II ANN software package. Training was generally complete after 100,000 iterations with the training set. Training times were in general less than 5 minutes in each case.

4.2 Neural Network Performance Evaluation

In this section, the identification performance of the ANN is evaluated in three ways. First, the neural network is trained with 100% of the training set, and then this training set is input to the ANN. A second test is performed where 50% of the events, which are chosen randomly, are used to train the ANN, and the remaining 50% are used for testing. A third test is performed where the ANN is first trained with 100% of the events, and then tested with signal parameters from the same events, but these parameters are estimated using 1, 5, 10, 15, and 20 NORESS array elements. This type of test provides some insight into the utility of the array over a single station.

4.2.1 100% Train/Test Experiment

In this experiment, the entire dataset of parameters from all 101 events was used to train the ANN. The number of iterations used during training was 100,000. After training, the dataset was processed by the ANN as a means of evaluation the class separation capability of the ANN. The results of this experiment are shown in *Table 3.* The ANN has correctly classified all but 2 of the explosions. These 2 explosions were misclassified as earthquakes. All of the earthquakes were correctly classified. No events were classified as *unknown*.

A standard way of presenting these results (standard in the classification and pattern recognition literature) is known as a *confusion matrix*. The matrix has on one of the horizontal axes the true classification of each event type in the training set (here, earthquake or explosion). On the other horizontal axis is the calculated event type (earthquake, explosion, or unknown). The vertical axis is the number of events in each box of the matrix. The confusion matrix for this experiment is shown in *Figure 26.* Another method is to plot the ANN output as a function of event number. This method shows not only the final classification but also the fit and separation of the classes of events. The neural network output for this experiment is shown in *Figure 27.*

Table 3. ANN Training/Testing for 100% of the dataset.

	Truth Class	
Computed Class	Explosion	Earthquake
Explosion	47	0
Earthquake	2	52
Unknown	0	0

4.2.2 50/50 Train/Test Experiment

For this second ANN experiment, 50% of the explosions and earthquakes in the training set were randomly selected. The signal parameters extracted from t hese events were then used to train the ANN with 100,000 iterations. After training, these same events were processed with the ANN. Table 4 shows that the ANN trained perfectly with this dataset; no events were misclassified by the ANN. A confusion matrix for this experiment is shown in *Figure 28.*

able 4. ANN Training for 50% of the dataset.		
	Truth Class	
Computed Class	Explosion	Earthquake
Explosion	25	0
Earthquake	0	26
Unknown	0	0

Next, the remaining 50% of the events were processed with the ANN. Here, the ANN is processing events that it has never seen before. *Table 5* shows that the ANN misclassified 5 of the explosions as earthquakes; 3 earthquakes were misclassified as explosions; 1 earthquake was classified as unknown.

Table 5. ANN Test for 50% of the dataset.		
	Truth Class	
Computed Class	Explosion	Earthquake
Explosion	21	3
Earthquake	5	22
Unknown	0	1

4.2.3 ANN Performance vs. Number of NORESS Elements

The advantage of an array of seismometers over a single station is well known from both theoretical and observational studies. The question we seek to answer here is how the ANN performance varies as a function of the number of array elements used to estimate the chosen signal parameters.

To accomplish this, each signal parameter for each event in the training database was calculated using 1, 5, 10, 15, and 20 NORESS elements (vertical channels only). These parameter sets were then input to the trained neural network. Output classifications were calculated, with the results presented in terms of both tables and confusion matrices.

For the 1-element recall (Table 6, Figure 30), the ANN has computed the correct classification for 42 of the explosions; 5 explosions were misclassified as earthquakes, and 2 explosions were classified as *unknown*. For the earthquakes, 36 events were correctly classified; 5 earthquakes were classified as explosions, and 2 earthquakes were classified as *unknown*.

Table 6. ANN Test for 1-Element Recall		
	Truth Class	
Computed Class	Explosion	Earthquake
Explosion	42	5
Earthquake	5	36
Unknown	2	2

For the 5-element recall (Table 7, Figure 31), the ANN has computed the correct classification for 42 of the explosions; 7 explosions were misclassified as earthquakes, and 0 explosions were classified as *unknown*. For the earthquakes, 50 events were correctly classified; 2 earthquakes were classified as *unknown*.

Table 7. ANN Test for 5-Element Recall		
	Truth Class	
Computed Class	Explosion	Earthquake
Explosion	42	0
Earthquake	7	50
Unknown	0	2

For the case of the 10-element recall (Table 8, Figure 32), the ANN has computed the correct classification for 41 of the explosions; 6 explosions were misclassified as earthquakes, and 2 explosions were classified as *unknown*. For the earthquakes, 51 events were correctly classified; 1 earthquake was classified as *unknown*.

Table 8. ANN Test for 10-Element Recall		
	Truth Class	
Computed Class	Explosion	Earthquake
Explosion	41	0
Earthquake	6	51
Unknown	2	1

For the 15-element recall (Table 9, Figure 33), the ANN has computed the correct classification for 44 of the explosions; 4 explosions were misclassified as earthquakes. For the earthquakes, all 52 events were correctly classified. None of the event were classified as *unknown*.

Table 9. ANN Test for 15-Element Recall		
	Truth Class	
Computed Class	Explosion	Earthquake
Explosion	41	0
Earthquake	0	52
Unknown	0	3

For the case of the 20-element recall (Table 10, Figure 34), the ANN has computed the correct classification for 44 of the explosions; 4 explosions were misclassified as earthquakes. For the earthquakes, all 52 events were correctly classified. None of the event were classified as ***unknown.***

Table 10. ANN Test for 20-Element Recall		
	Truth Class	
Computed Class	Explosion	Earthquake
Explosion	45	0
Earthquake	4	52
Unknown	0	0

Another way of presenting this information is in terms of a receiver operating characteristic (ROC) curve. *Figure 35* shows the percent of correct classifications for the above tests as a function of the number of NORESS elements used. *Figure 36* shows the number of misidentifications as a function of the number of NORESS elements used. The number of misidentifications decreases from 23 when 1 element is used, to 2 when 25 elements are used. Finally, *Figure 37* shows the RMS recall error for the classifications (model misfits) versus the number of NORESS elements used. In all of these cases, we have seen the advantage of the total array estimate of the signal parameters over a single element or array subset, which basically confirms the increase in the SNR for increasing numbers of channels.

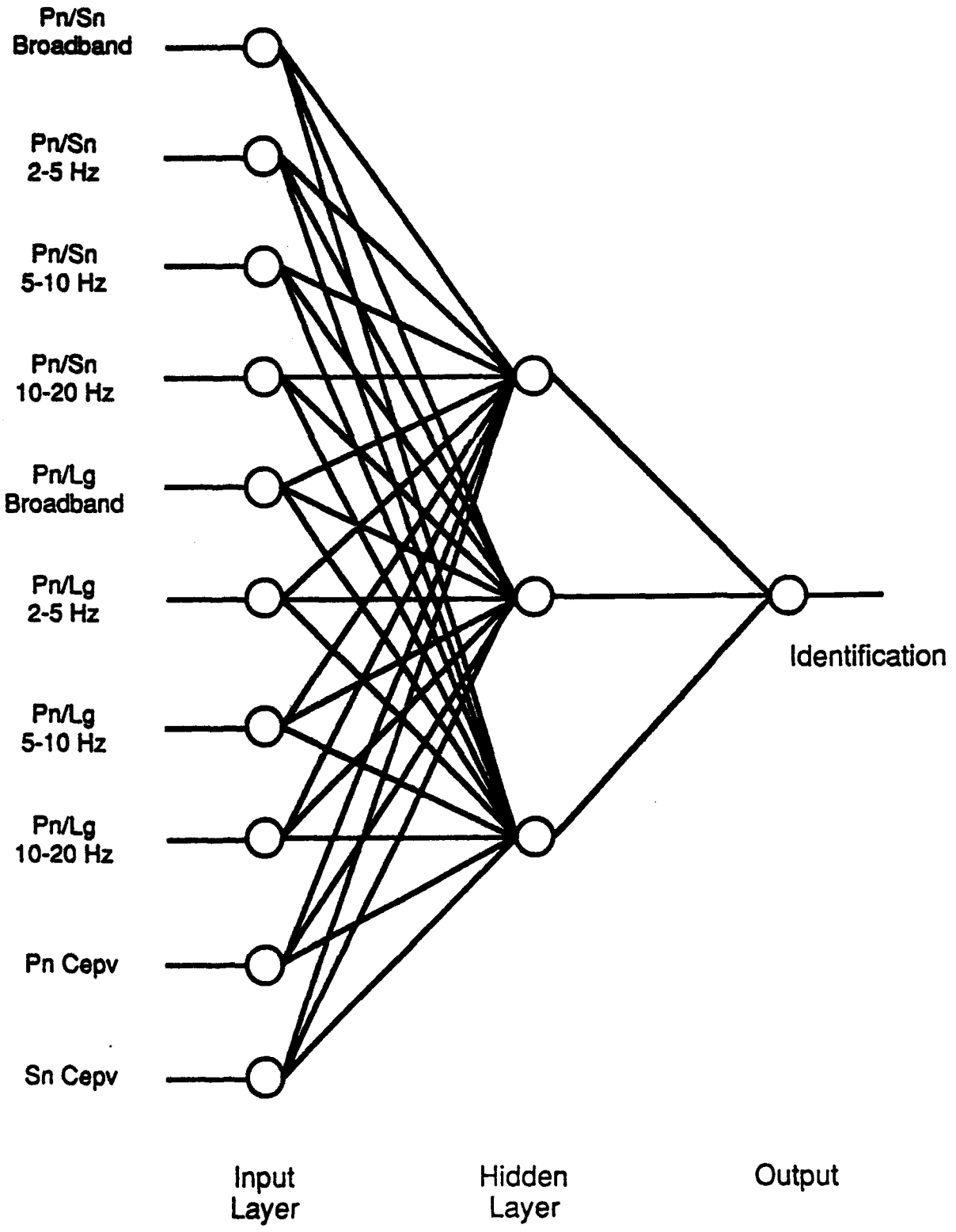

Figure 25. Backpropagation ANN architecture used in this study.

Confusion Matrix for 100% of Events

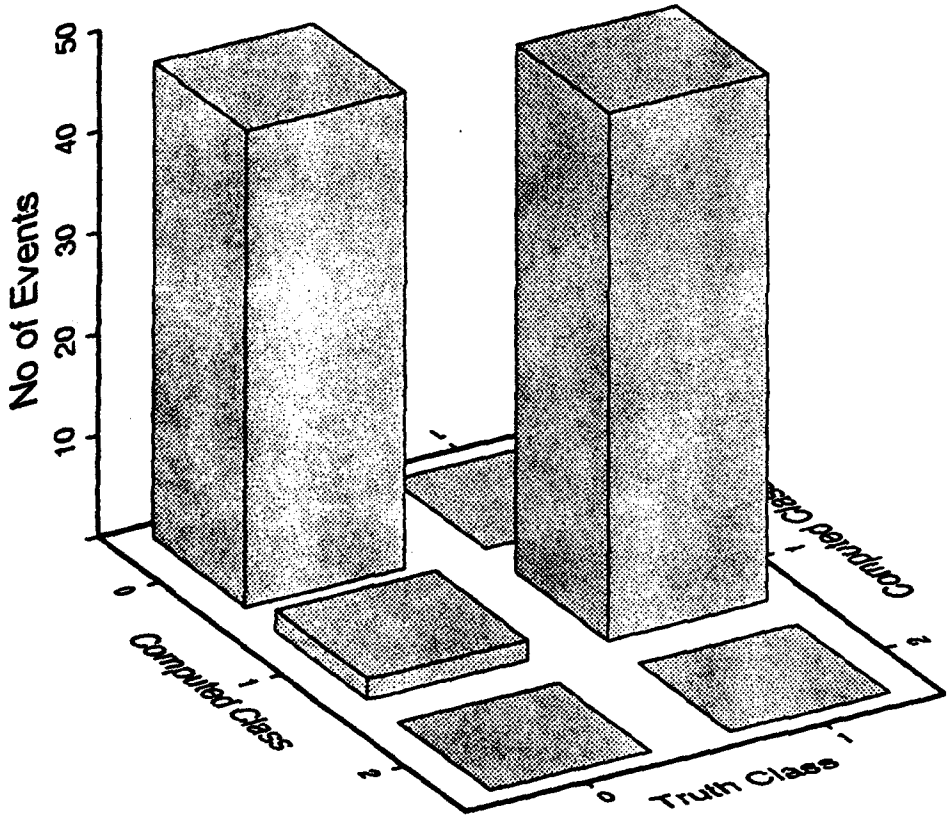

Class 0 Explo, Class 1 Equake, Class 2 Unknown

Figure 26. Confusion matrix for the ANN classification using 100% of the events.

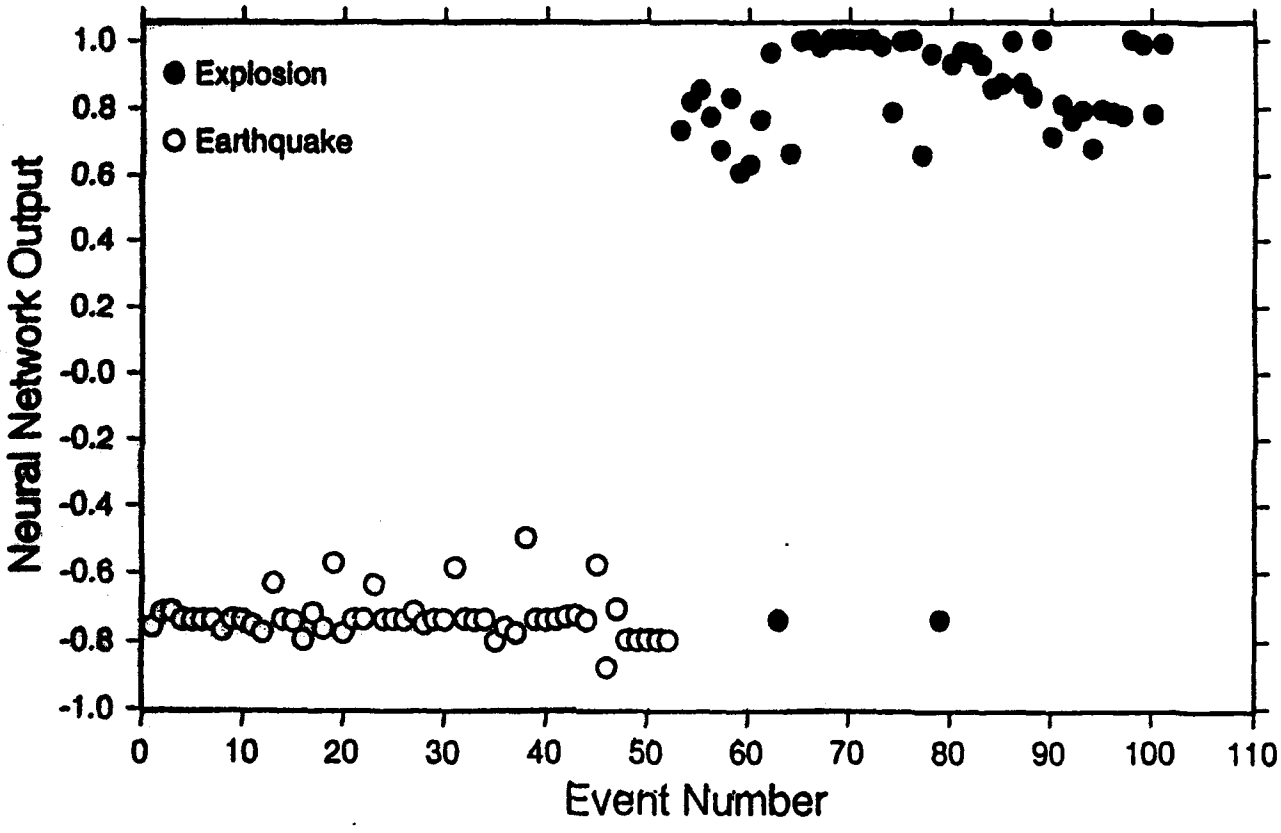

Figure 27. ANN output for each event in the 100% train/test experiment.

Confusion Matrix for 50% of Events

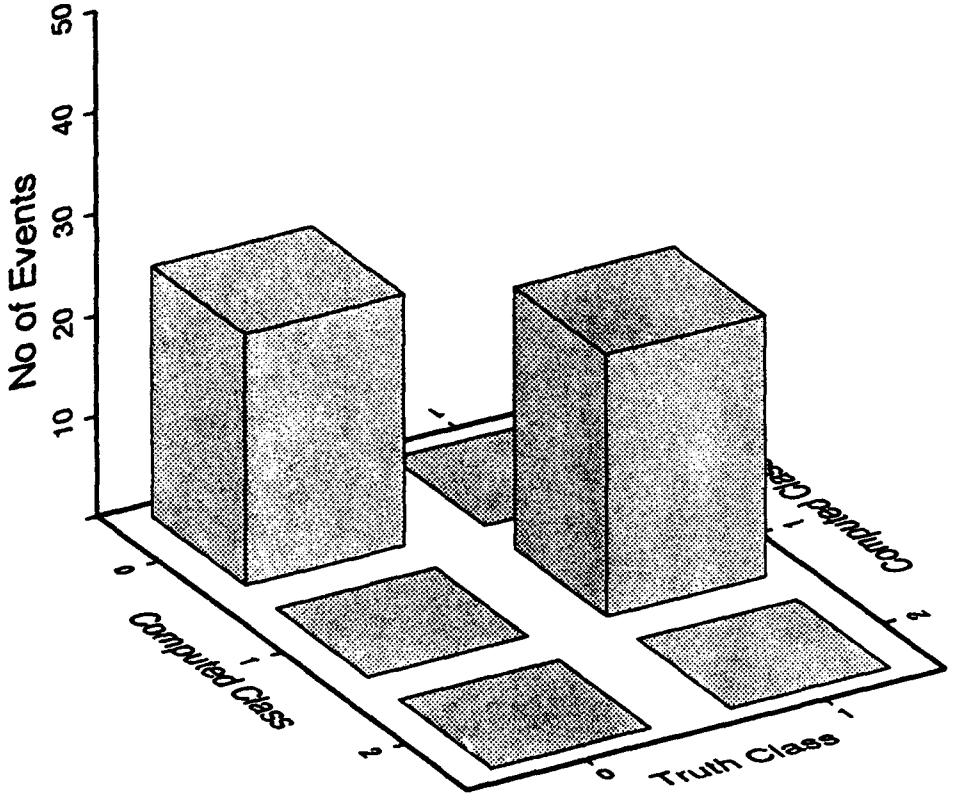

Class 0 Explo, Class 1 Equake, Class 2 Unknown

Figure 28. Confusion matrix for the 50% training experiment.

Confusion Matrix for 50% of Test Events

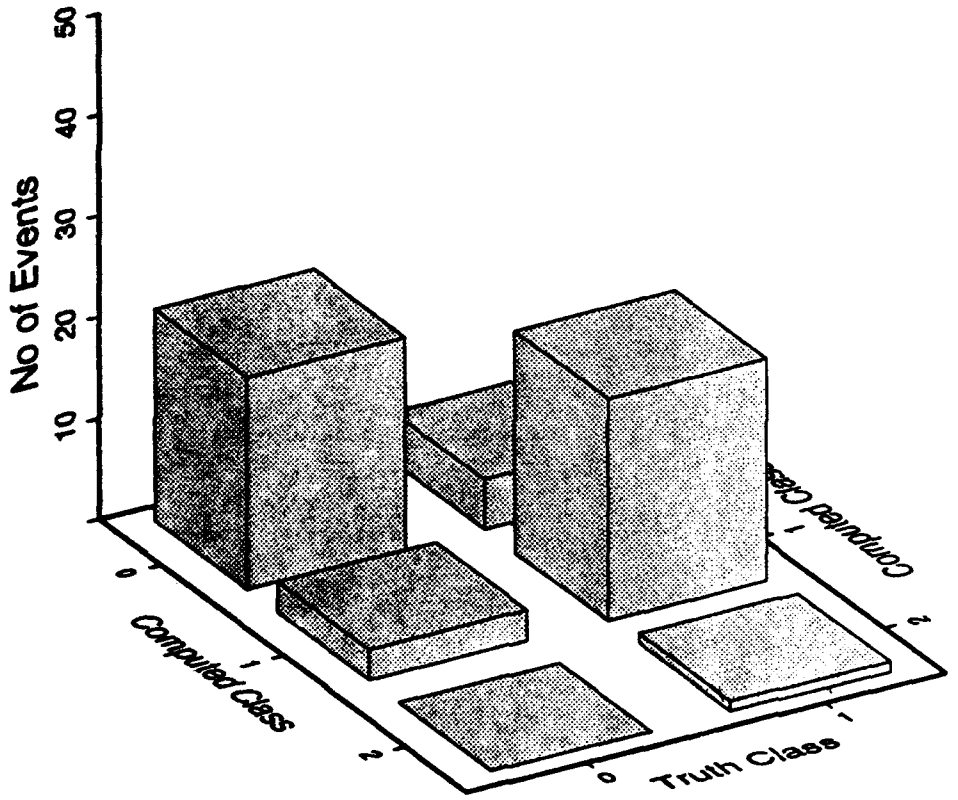

Class 0 Explo, Class 1 Equake, Class 2 Unknown

Figure 29. Confusion matrix for the 50% test experiment.

Confusion Matrix for 1 Station Recall

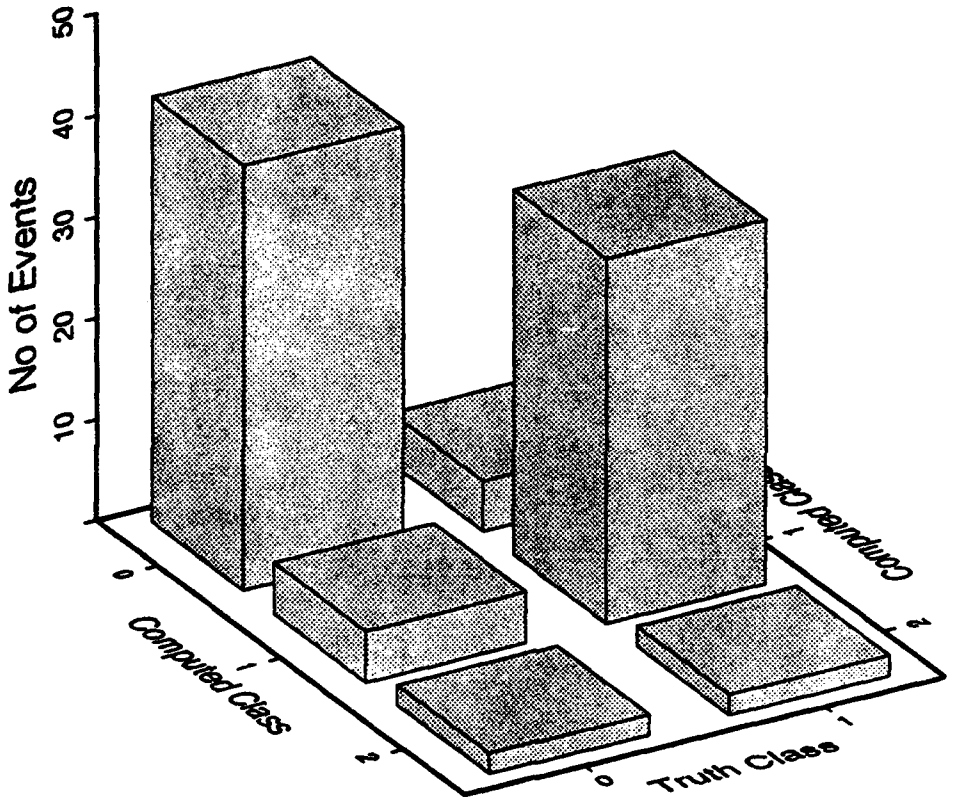

Class 0 Explo, Class 1 Equake, Class 2 Unknown

Figure 30. Confusion matrix for ANN classification using 1 NORESS station.

Confusion Matrix for 5 Station Recall

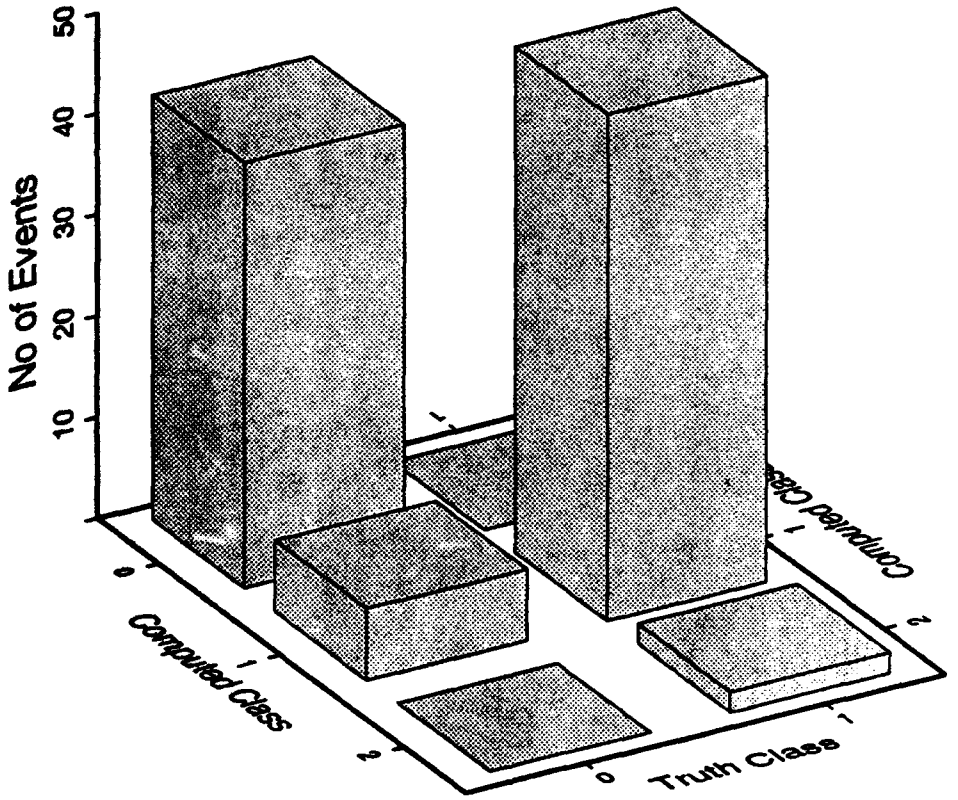

Class 0 Explo, Class 1 Equake, Class 2 Unknown

Figure 31. Confusion matrix for ANN classification using 5 NORESS stations.

Confusion Matrix for 10 Station Recall

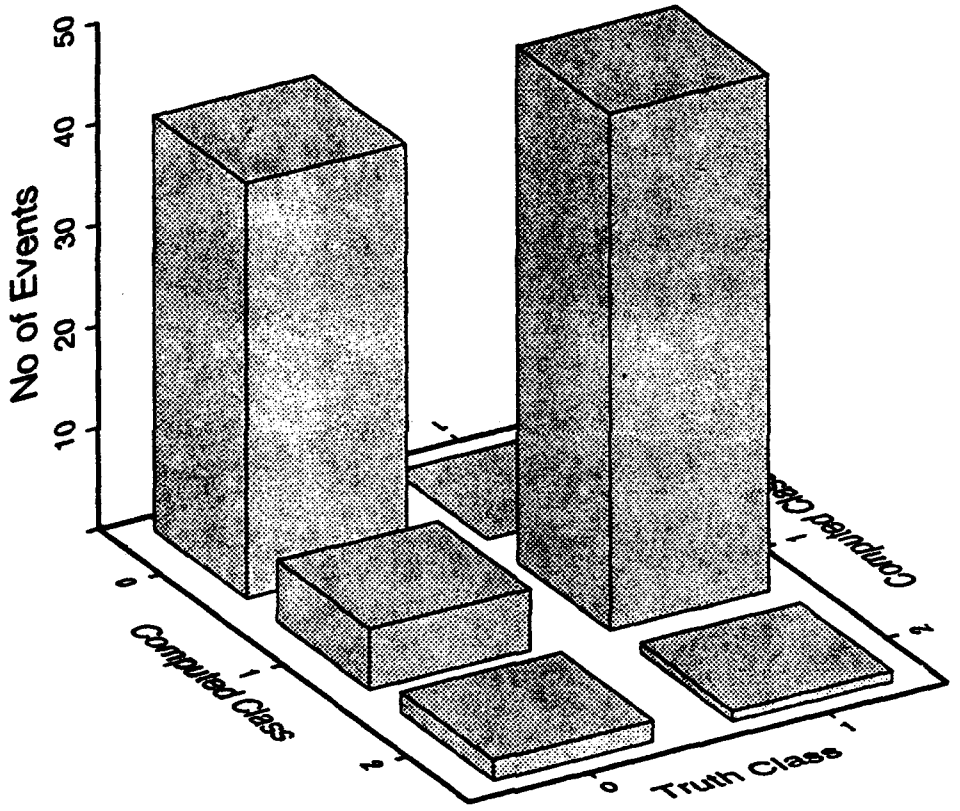

Class 0 Explo, Class 1 Equake, Class 2 Unknown

Figure 32. Confusion matrix for ANN classification using 10 NORESS stations.

Confusion Matrix for 15 Station Recall

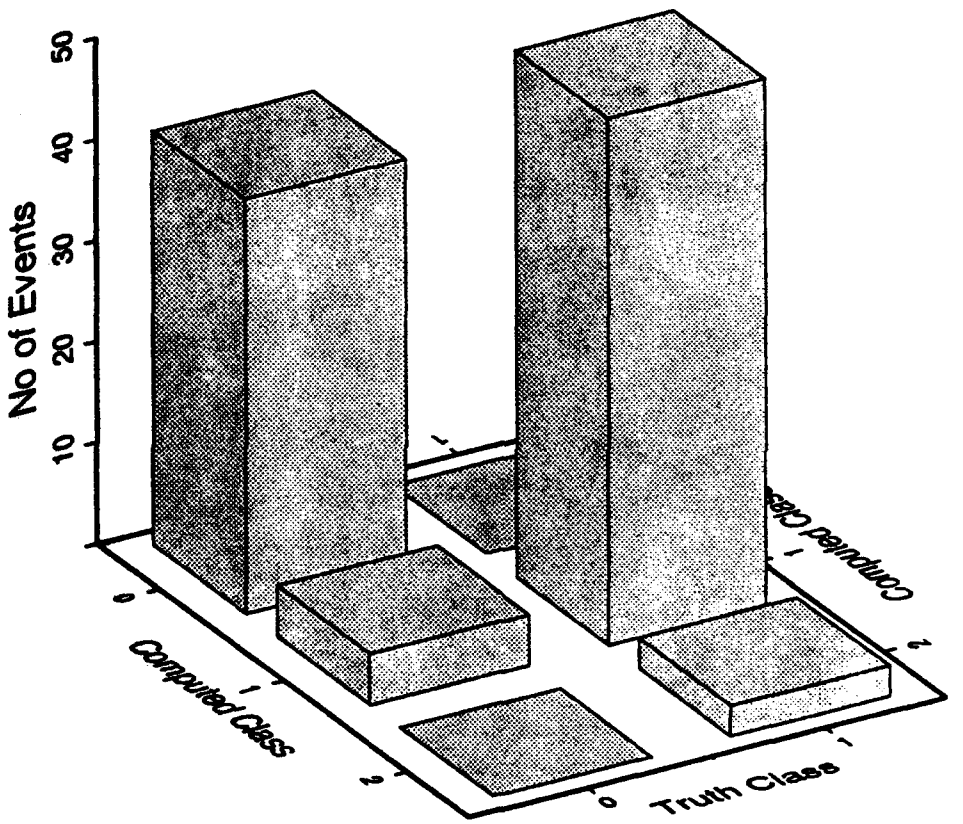

Class 0 Explo, Class 1 Equake, Class 2 Unknown

Figure 33. Confusion matrix for ANN classification using 15 NORESS stations.

Confusion Matrix for 20 Station Recall

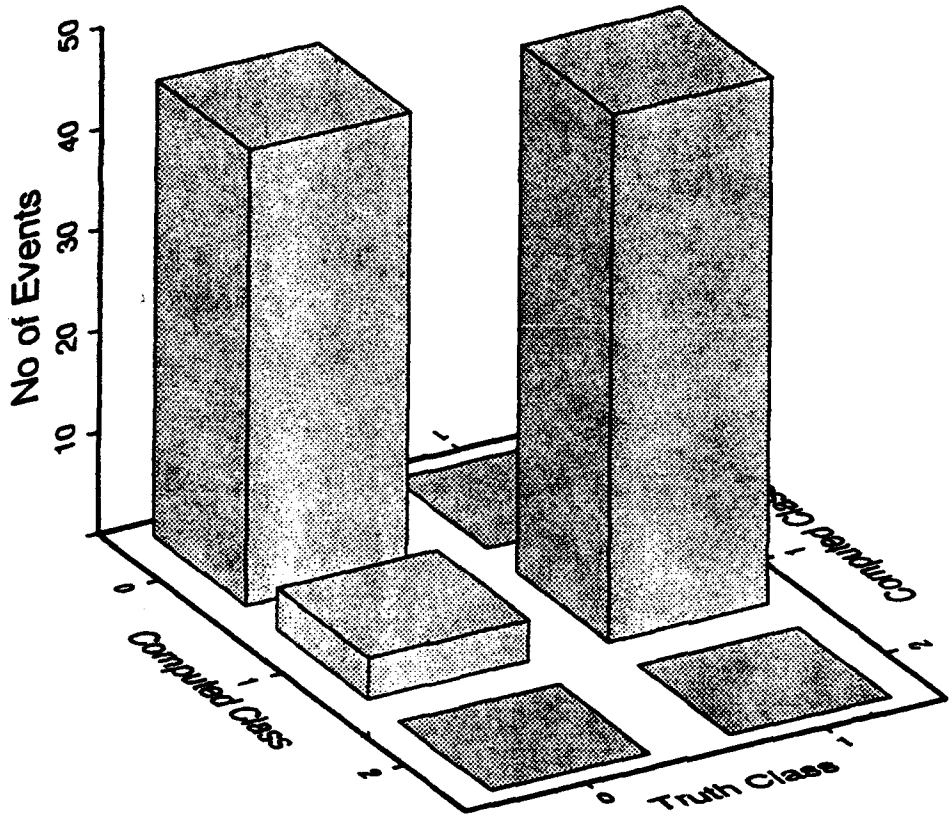

Class 0 Explo, Class 1 Equake, Class 2 Unknown

Figure 34. Confusion matrix for ANN classification using 20 NORESS stations.

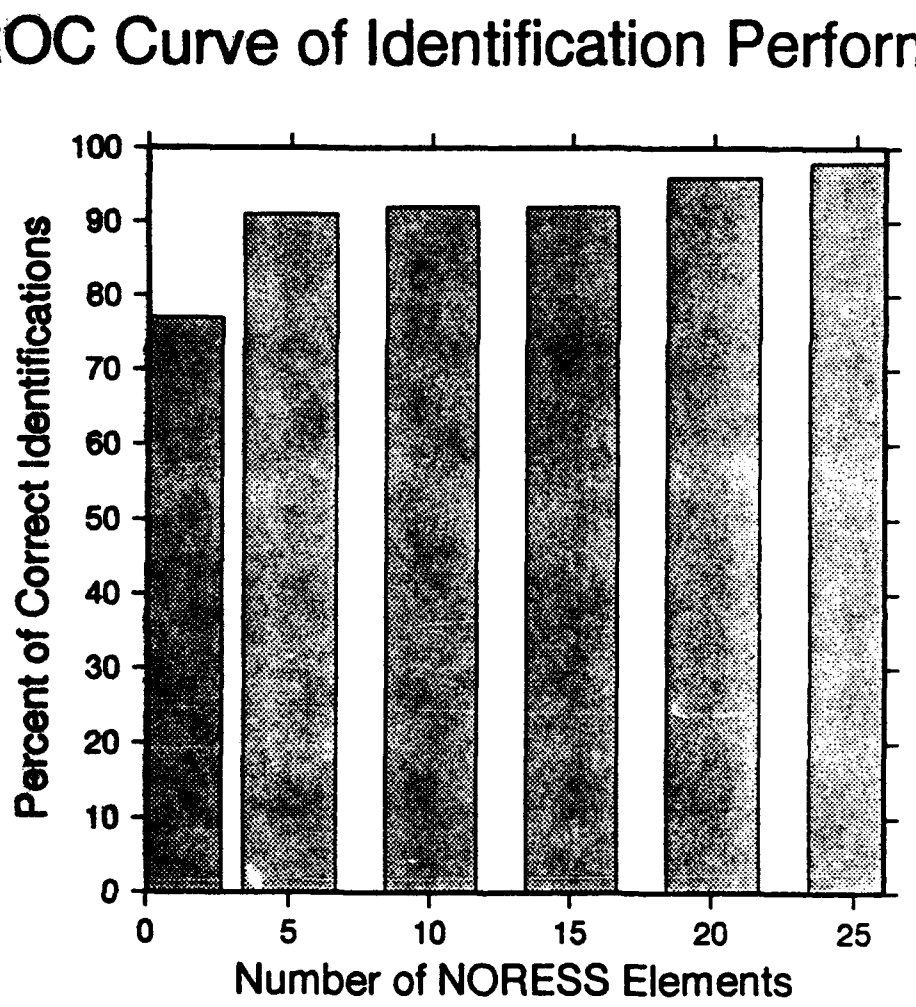

Figure 35. **ROC curve of identification performance vs. number of NORESS stations.**

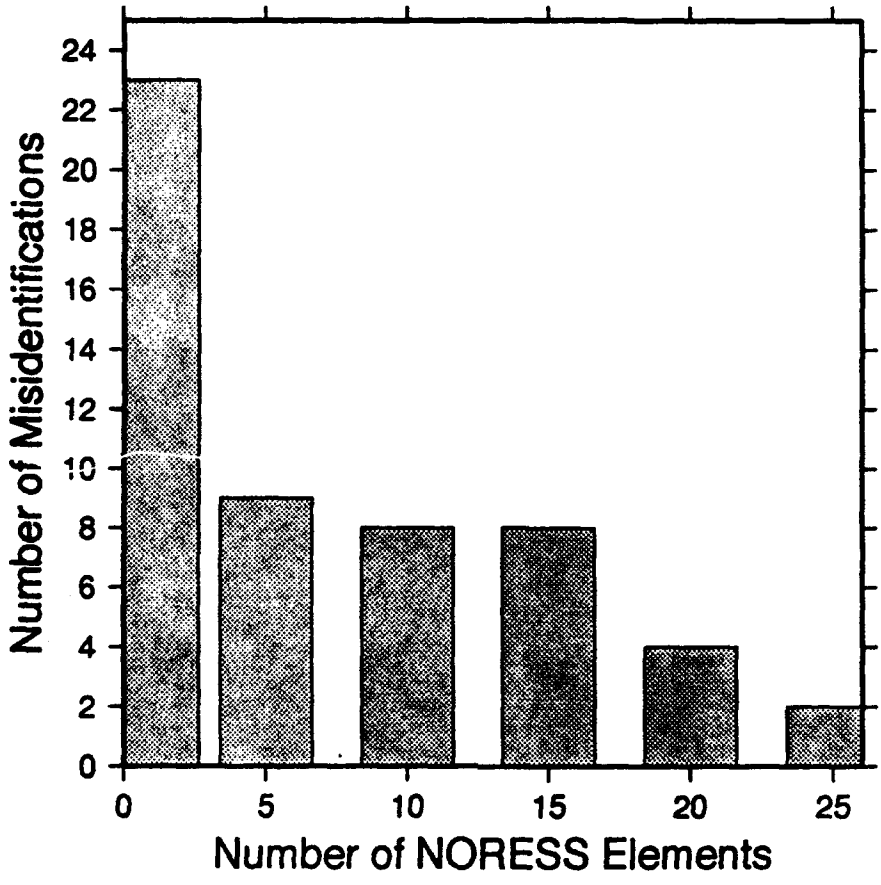

Figure 36. Misidentifications as a function of the number of NORESS stations.

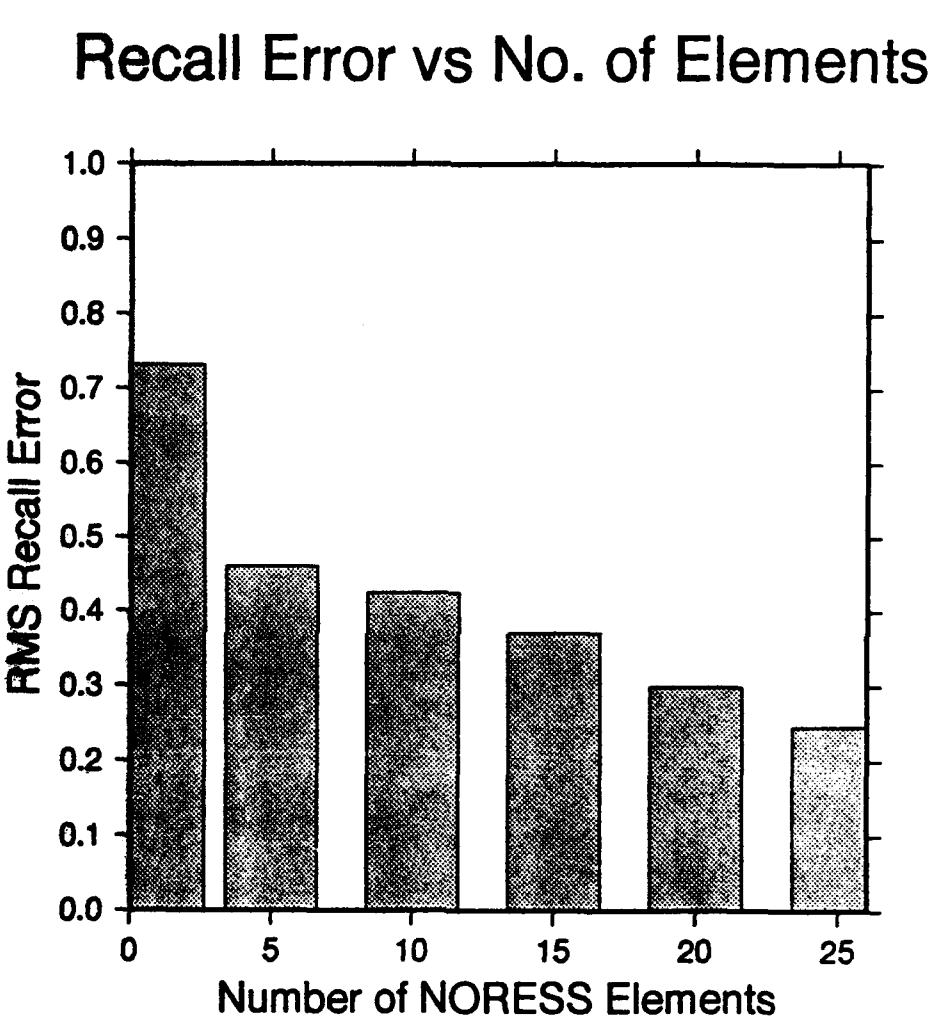

Figure 37. **RMS recall error as a function of the number of NORESS stations.**

5. Summary and Conclusions

The objective of this research was to test the applicability of machine learning techniques (specifically backpropagation artificial neural networks) to the problem of small seismic event identification. The results indicate that the ANN's are an effective tool for this job, and we believe that the ANN approach should be tested further as part of an online identification system. The classifications produced by the ANN can be either compared to those of a trained analyst, compared with the classifications produced by the expert system (IMS), or combined with all of the classifications using a fuzzy logic approach.

Specifically, our research has shown the following:

- Statistical analysis of the chosen signal parameters indicates that the most important parameters for small event identification in the Scandinavian area are:
  - Broadband P_n/S_n spectral ratio
  - P_n and S_n cepstral variance
  - P_n/L_g spectral ratio from 5-10 Hz
  - P_n/L_g spectral ratio from 2-5 Hz
  - P_n/S_n spectral ratio from 2-5 Hz
  - P_n/L_g spectral ratio from 10-20 Hz

- When the ANN is trained with all of the examples, the separation of the classes is correct for all but 2 of the events. The ANN misclassified 2 explosions as earthquakes.

- In a test where the ANN was trained with 50% of the events, randomly selected, the ANN correctly classified 21 of the 26 explosions correctly. The ANN classified 22 of the 26 earthquakes correctly.

- Using just the single central vertical array element of NORESS, the ANN correctly classifies 77% of the 101 events in our training set.

- Using all 25 elements of the NORESS array, the ANN correctly classifies 98% of our training events.

6. References

Bache, T.C., S.R. Bratt, J. Wang, R.M. Fung, C. Kobryn, and J.W. Given (1990), The Intelligent Monitoring System, *Bull. Seis. Soc. Amer., 80,* 1833-1851.

Blandford, R., A. Dainty, R. Lacoss, R. Maxion, A. Ryall, B. Stump, C. Thurber, and T. Wallace (1992), Report on the DARPA Seismic Identification Workshop, DARPA publication, 28 pp.

Bratt, S.R., H.J. Swanger, R.J. Stead, F. Ryall, and T.C. Bache (1990), Initial results from the Intelligent Monitoring System, *Bull. Seis. Soc. Amer., 80,* 1852-1873.

Cattell, R.B. (1966), The SCREE test for the number of factors, *Mult. Behav. Res., 1,* 245-276.

Dysart, P.S. and Pulli, J.J. (1990), Regional seismic event classification at the NORESS array: seismological measurements and the use of trained neural networks, *Bull. Seis. Soc. Amer., 60,* 109-129.

Enslein, K., Ralston, A., and Wilf, H. S. (Eds.), Statistical Methods for Digital Computers, Vol. 3, Wiley & Sons, Inc., 1977.

Grant, L. and J. Coyne (1992), Ground truth data for seismic discrimination research, Proc. 14th Annual PL/DARPA Seismic Research Symposium, 139-145. PL-TR-92-2210

Jackson, J.E., A User's Guide To Principal Components, Wiley & Sons, Inc., 1991.

Klimasauskas, C. and P. DuBose, (1990), Applying Neural Computing in Business, Industry, and Government, Seminar Notes, NeuralWare Inc., Pittsburg, PA, 199.

Lacoss, R.T., S.R. Curtis, and R.K. Cunningham (1992), Seismic phase and event recognition using algorithms that learn from examples, Proc. 14th Annual PL/DARPA Seismic Research Symposium, 267-273. PL-TR-92-2210

Lippman, R. (1987), An introduction to computing with neural nets, *IEEE ASSP Magazine.*

Sereno, T. and G. Patnaik (1991), Data to test and evaluate the performance of neural network architectures for seismic signal discrimination, PL-TR-92-2110(I) ADA254413

DISTRIBUTION LIST

Prof. Thomas Ahrens
Seismological Lab, 252-21
Division of Geological & Planetary Sciences
California Institute of Technology
Pasadena, CA 91125

Prof. Keiiti Aki
Center for Earth Sciences
University of Southern California
University Park
Los Angeles, CA 90089-0741

Prof. Shelton Alexander
Geosciences Department
403 Deike Building
The Pennsylvania State University
University Park, PA 16802

Dr. Ralph Alewine, III
DARPA/NMRO
3701 North Fairfax Drive
Arlington, VA 22203-1714

Prof. Charles B. Archambeau
CIRES
University of Colorado
Boulder, CO 80309

Dr. Thomas C. Bache, Jr.
Science Applications Int'l Corp.
10260 Campus Point Drive
San Diego, CA 92121 (2 copies)

Prof. Muawia Barazangi
Institute for the Study of the Continent
Cornell University
Ithaca, NY 14853

Dr. Jeff Barker
Department of Geological Sciences
State University of New York
at Binghamton
Vestal, NY 13901

Dr. Douglas R. Baumgardt
ENSCO, Inc
5400 Port Royal Road
Springfield, VA 22151-2388

Dr. Susan Beck
Department of Geosciences
Building #77
University of Arizona
Tuscon, AZ 85721

Dr. T.J. Bennett
S-CUBED
A Division of Maxwell Laboratories
11800 Sunrise Valley Drive, Suite 1212
Reston, VA 22091

Dr. Robert Blandford
AFTAC/TT, Center for Seismic Studies
1300 North 17th Street
Suite 1450
Arlington, VA 22209-2308

Dr. G.A. Bollinger
Department of Geological Sciences
Virginia Polytechnical Institute
21044 Derring Hall
Blacksburg, VA 24061

Dr. Stephen Bratt
Center for Seismic Studies
1300 North 17th Street
Suite 1450
Arlington, VA 22209-2308

Dr. Lawrence Burdick
Woodward-Clyde Consultants
566 El Dorado Street
Pasadena, CA 91109-3245

Dr. Robert Burridge
Schlumberger-Doll Research Center
Old Quarry Road
Ridgefield, CT 06877

Dr. Jerry Carter
Center for Seismic Studies
1300 North 17th Street
Suite 1450
Arlington, VA 22209-2308

Dr. Eric Chael
Division 9241
Sandia Laboratory
Albuquerque, NM 87185

Prof. Vernon F. Cormier
Department of Geology & Geophysics
U-45, Room 207
University of Connecticut
Storrs, CT 06268

Prof. Steven Day
Department of Geological Sciences
San Diego State University
San Diego, CA 92182

Marvin Denny
U.S. Department of Energy
Office of Arms Control
Washington, DC 20585

Dr. Zoltan Der
ENSCO, Inc.
5400 Port Royal Road
Springfield, VA 22151-2388

Prof. Adam Dziewonski
Hoffman Laboratory, Harvard University
Dept. of Earth Atmos. & Planetary Sciences
20 Oxford Street
Cambridge, MA 02138

Prof. John Ebel
Department of Geology & Geophysics
Boston College
Chestnut Hill, MA 02167

Eric Fielding
SNEE Hall
INSTOC
Cornell University
Ithaca, NY 14853

Dr. Mark D. Fisk
Mission Research Corporation
735 State Street
P.O. Drawer 719
Santa Barbara, CA 93102

Prof Stanley Flatte
Applied Sciences Building
University of California, Santa Cruz
Santa Cruz, CA 95064

Dr. John Foley
NER-Geo Sciences
1100 Crown Colony Drive
Quincy, MA 02169

Prof. Donald Forsyth
Department of Geological Sciences
Brown University
Providence, RI 02912

Dr. Art Frankel
U.S. Geological Survey
922 National Center
Reston, VA 22092

Dr. Cliff Frolich
Institute of Geophysics
8701 North Mopac
Austin, TX 78759

Dr. Holly Given
IGPP, A-025
Scripps Institute of Oceanography
University of California, San Diego
La Jolla, CA 92093

Dr. Jeffrey W. Given
SAIC
10260 Campus Point Drive
San Diego, CA 92121

Dr. Dale Glover
Defense Intelligence Agency
ATTN: ODT-1B
Washington, DC 20301

Dr. Indra Gupta
Teledyne Geotech
314 Montgomery Street
Alexanderia, VA 22314

Dan N. Hagedon
Pacific Northwest Laboratories
Battelle Boulevard
Richland, WA 99352

Dr. James Hannon
Lawrence Livermore National Laboratory
P.O. Box 808
L-205
Livermore, CA 94550

Dr. Roger Hansen
HQ AFTAC/TTR
Patrick AFB, FL 32925-6001

Prof. David G. Harkrider
Seismological Laboratory
Division of Geological & Planetary Sciences
California Institute of Technology
Pasadena, CA 91125

Prof. Danny Harvey
CIRES
University of Colorado
Boulder, CO 80309

Prof. Donald V. Helmberger
Seismological Laboratory
Division of Geological & Planetary Sciences
California Institute of Technology
Pasadena, CA 91125

Prof. Eugene Herrin
Institute for the Study of Earth and Man
Geophysical Laboratory
Southern Methodist University
Dallas, TX 75275

Prof. Robert B. Herrmann
Department of Earth & Atmospheric Sciences
St. Louis University
St. Louis, MO 63156

Prof. Lane R. Johnson
Seismographic Station
University of California
Berkeley, CA 94720

Prof. Thomas H. Jordan
Department of Earth, Atmospheric &
Planetary Sciences
Massachusetts Institute of Technology
Cambridge, MA 02139

Prof. Alan Kafka
Department of Geology & Geophysics
Boston College
Chestnut Hill, MA 02167

Robert C. Kemerait
ENSCO, Inc.
445 Pineda Court
Melbourne, FL 32940

Dr. Max Koontz
U.S. Dept. of Energy/DP 5
Forrestal Building
1000 Independence Avenue
Washington, DC 20585

Dr. Richard LaCoss
MIT Lincoln Laboratory, M-200B
P.O. Box 73
Lexington, MA 02173-0073

Dr. Fred K. Lamb
University of Illinois at Urbana-Champaign
Department of Physics
1110 West Green Street
Urbana, IL 61801

Prof. Charles A. Langston
Geosciences Department
403 Deike Building
The Pennsylvania State University
University Park, PA 16802

Jim Lawson, Chief Geophysicist
Oklahoma Geological Survey
Oklahoma Geophysical Observatory
P.O. Box 8
Leonard, OK 74043-0008

Prof. Thorne Lay
Institute of Tectonics
Earth Science Board
University of California, Santa Cruz
Santa Cruz, CA 95064

Dr. William Leith
U.S. Geological Survey
Mail Stop 928
Reston, VA 22092

Mr. James F. Lewkowicz
Phillips Laboratory/GPEH
Hanscom AFB, MA 01731-5000(2 copies)

Mr. Alfred Lieberman
ACDA/VI-OA State Department Building
Room 5726
320-21st Street, NW
Washington, DC 20451

Prof. L. Timothy Long
School of Geophysical Sciences
Georgia Institute of Technology
Atlanta, GA 30332

Dr. Randolph Martin, III
New England Research, Inc.
76 Olcott Drive
White River Junction, VT 05001

Dr. Robert Masse
Denver Federal Building
Box 25046, Mail Stop 967
Denver, CO 80225

Dr. Gary McCartor
Department of Physics
Southern Methodist University
Dallas, TX 75275

Prof. Thomas V. McEvilly
Seismographic Station
University of California
Berkeley, CA 94720

Dr. Art McGarr
U.S. Geological Survey
Mail Stop 977
U.S. Geological Survey
Menlo Park, CA 94025

Dr. Keith L. McLaughlin
S-CUBED
A Division of Maxwell Laboratory
P.O. Box 1620
La Jolla, CA 92038-1620

Stephen Miller & Dr. Alexander Florence
SRI International
333 Ravenswood Avenue
Box AF 116
Menlo Park, CA 94025-3493

Prof. Bernard Minster
IGPP, A-025
Scripps Institute of Oceanography
University of California, San Diego
La Jolla, CA 92093

Prof. Brian J. Mitchell
Department of Earth & Atmospheric Sciences
St. Louis University
St. Louis, MO 63156

Mr. Jack Murphy
S-CUBED
A Division of Maxwell Laboratory
11800 Sunrise Valley Drive, Suite 1212
Reston, VA 22091 (2 Copies)

Dr. Keith K. Nakanishi
Lawrence Livermore National Laboratory
L-025
P.O. Box 808
Livermore, CA 94550

Dr. Carl Newton
Los Alamos National Laboratory
P.O. Box 1663
Mail Stop C335, Group ESS-3
Los Alamos, NM 87545

Dr. Bao Nguyen
HQ AFTAC/TTR
Patrick AFB, FL 32925-6001

Prof. John A. Orcutt
IGPP, A-025
Scripps Institute of Oceanography
University of California, San Diego
La Jolla, CA 92093

Prof. Jeffrey Park
Kline Geology Laboratory
P.O. Box 6666
New Haven, CT 06511-8130

Dr. Howard Patton
Lawrence Livermore National Laboratory
L-025
P.O. Box 808
Livermore, CA 94550

Dr. Frank Pilotte
HQ AFTAC/TT
Patrick AFB, FL 32925-6001

Dr. Jay J. Pulli
Radix Systems, Inc.
2 Taft Court, Suite 203
Rockville, MD 20850

Dr. Robert Reinke
ATTN: FCTVTD
Field Command
Defense Nuclear Agency
Kirtland AFB, NM 87115

Prof. Paul G. Richards
Lamont-Doherty Geological Observatory
of Columbia University
Palisades, NY 10964

Mr. Wilmer Rivers
Teledyne Geotech
314 Montgomery Street
Alexandria, VA 22314

Dr. George Rothe
HQ AFTAC/TTR
Patrick AFB, FL 32925-6001

Dr. Alan S. Ryall, Jr.
DARPA/NMRO
3701 North Fairfax Drive
Arlington, VA 22209-1714

Dr. Richard Sailor
TASC, Inc.
55 Walkers Brook Drive
Reading, MA 01867

Prof. Charles G. Sammis
Center for Earth Sciences
University of Southern California
University Park
Los Angeles, CA 90089-0741

Prof. Christopher H. Scholz
Lamont-Doherty Geological Observatory
of Columbia University
Palisades, NY 10964

Dr. Susan Schwartz
Institute of Tectonics
1156 High Street
Santa Cruz, CA 95064

Secretary of the Air Force
(SAFRD)
Washington, DC 20330

Office of the Secretary of Defense
DDR&E
Washington, DC 20330

Thomas J. Sereno, Jr.
Science Application Int'l Corp.
10260 Campus Point Drive
San Diego, CA 92121

Dr. Michael Shore
Defense Nuclear Agency/SPSS
6801 Telegraph Road
Alexandria, VA 22310

Dr. Matthew Sibol
Virginia Tech
Seismological Observatory
4044 Derring Hall
Blacksburg, VA 24061-0420

Prof. David G. Simpson
IRIS, Inc.
1616 North Fort Myer Drive
Suite 1440
Arlington, VA 22209

Donald L. Springer
Lawrence Livermore National Laboratory
L-025
P.O. Box 808
Livermore, CA 94550

Dr. Jeffrey Stevens
S-CUBED
A Division of Maxwell Laboratory
P.O. Box 1620
La Jolla, CA 92038-1620

Lt. Col. Jim Stobie
ATTN: AFOSR/NL
Bolling AFB
Washington, DC 20332-6448

Prof. Brian Stump
Institute for the Study of Earth & Man
Geophysical Laboratory
Southern Methodist University
Dallas, TX 75275

Prof. Jeremiah Sullivan
University of Illinois at Urbana-Champaign
Department of Physics
1110 West Green Street
Urbana, IL 61801

Prof. L. Sykes
Lamont-Doherty Geological Observatory
of Columbia University
Palisades, NY 10964

Dr. David Taylor
ENSCO, Inc.
445 Pineda Court
Melbourne, FL 32940

Dr. Steven R. Taylor
Los Alamos National Laboratory
P.O. Box 1663
Mail Stop C335
Los Alamos, NM 87545

Prof. Clifford Thurber
University of Wisconsin-Madison
Department of Geology & Geophysics
1215 West Dayton Street
Madison, WS 53706

Prof. M. Nafi Toksoz
Earth Resources Lab
Massachusetts Institute of Technology
42 Carleton Street
Cambridge, MA 02142

Dr. Larry Turnbull
CIA-OSWR/NED
Washington, DC 20505

Dr. Gregory van der Vink
IRIS, Inc.
1616 North Fort Myer Drive
Suite 1440
Arlington, VA 22209

Dr. Karl Veith
EG&G
5211 Auth Road
Suite 240
Suitland, MD 20746

Prof. Terry C. Wallace
Department of Geosciences
Building #77
University of Arizona
Tuscon, AZ 85721

Dr. Thomas Weaver
Los Alamos National Laboratory
P.O. Box 1663
Mail Stop C335
Los Alamos, NM 87545

Dr. William Wortman
Mission Research Corporation
8560 Cinderbed Road
Suite 700
Newington, VA 22122

Prof. Francis T. Wu
Department of Geological Sciences
State University of New York
at Binghamton
Vestal, NY 13901

AFTAC/CA
(STINFO)
Patrick AFB, FL 32925-6001

DARPA/PM
3701 North Fairfax Drive
Arlington, VA 22203-1714

DARPA/RMO/RETRIEVAL
3701 North Fairfax Drive
Arlington, VA 22203-1714

DARPA/RMO/SECURITY OFFICE
3701 North Fairfax Drive
Arlington, VA 22203-1714

HQ DNA
ATTN: Technical Library
Washington, DC 20305

Defense Intelligence Agency
Directorate for Scientific & Technical Intelligence
ATTN: DTIB
Washington, DC 20340-6158

Defense Technical Information Center
Cameron Station
Alexandria, VA 22314 (2 Copies)

TACTEC
Battelle Memorial Institute
505 King Avenue
Columbus, OH 43201 (Final Report)

Phillips Laboratory
ATTN: XPG
Hanscom AFB, MA 01731-5000

Phillips Laboratory
ATTN: GPE
Hanscom AFB, MA 01731-5000

Phillips Laboratory
ATTN: TSML
Hanscom AFB, MA 01731-5000

Phillips Laboratory
ATTN: SUL
Kirtland, NM 87117 (2 copies)

Dr. Michel Bouchon
I.R.I.G.M.-B.P. 68
38402 St. Martin D'Heres
Cedex, FRANCE

Dr. Michel Campillo
Observatoire de Grenoble
I.R.I.G.M.-B.P. 53
38041 Grenoble, FRANCE

Dr. Kin Yip Chun
Geophysics Division
Physics Department
University of Toronto
Ontario, CANADA

Prof. Hans-Peter Harjes
Institute for Geophysic
Ruhr University/Bochum
P.O. Box 102148
4630 Bochum 1, GERMANY

Prof. Eystein Husebye
NTNF/NORSAR
P.O. Box 51
N-2007 Kjeller, NORWAY

David Jepsen
Acting Head, Nuclear Monitoring Section
Bureau of Mineral Resources
Geology and Geophysics
G.P.O. Box 378, Canberra, AUSTRALIA

Ms. Eva Johannisson
Senior Research Officer
National Defense Research Inst.
P.O. Box 27322
S-102 54 Stockholm, SWEDEN

Dr. Peter Marshall
Procurement Executive
Ministry of Defense
Blacknest, Brimpton
Reading FG7-FRS, UNITED KINGDOM

Dr. Bernard Massinon, Dr. Pierre Mechler
Societe Radiomana
27 rue Claude Bernard
75005 Paris, FRANCE (2 Copies)

Dr. Svein Mykkeltveit
NTNT/NORSAR
P.O. Box 51
N-2007 Kjeller, NORWAY (3 Copies)

Prof. Keith Priestley
University of Cambridge
Bullard Labs, Dept. of Earth Sciences
Madingley Rise, Madingley Road
Cambridge CB3 OEZ, ENGLAND

Dr. Jorg Schlittenhardt
Federal Institute for Geosciences & Nat'l Res.
Postfach 510153
D-3000 Hannover 51, GERMANY

Dr. Johannes Schweitzer
Institute of Geophysics
Ruhr University/Bochum
P.O. Box 1102148
4360 Bochum 1, GERMANY